6 Magnetism

C. M. SORENSEN

Department of Physics, Kansas State
University, Manhattan, Kansas

6.1 INTRODUCTION

Magnetism and magnetic phenomena are well known to all of us, scientist and layperson alike. If we are technically inclined, we come to realize that magnets are important for motors, actuators, information storage media, electrical power trans¬formation, electronic circuits, ferrofluids, and medical applications. A deeper look into the science of magnetism shows us that it is a remarkably rich and multifaceted area of study. Thus it is a daunting task to summarize and explain this vast and detailed field in one chapter.

The intent here is to review aspects of magnetism that the author has personally found useful and necessary in research involving nanoparticle magnetism. Thus this is not so much a chapter on nanoscale magnetism, but rather a chapter describing what you need to know to do nanoscale magnetism. Throughout this chapter three excellent references have been drawn upon extensively: the book by Cullity, now a classic in its field; Kittel's2 chapters on magnetism in his solid state physics book; and the very accessible book by Jiles.3 Any of

---

6 Từ học checked 6 h 17 1/4

CM Sorensen

Khoa Vật lý, Đại học bang Kansas Manhattan, Kansas

6.1 GIỚI THIỆU

Từ học và hiện tượng từ là những khái niệm rất quen thuộc đối với tất cả chúng ta, các nhà khoa học cũng như những người không chuyên môn. Nếu chúng ta học về kỹ thuật, chúng ta sẽ nhận thấy rằng nam châm có vai trò quan trọng trong mô-tơ, cơ cấu truyền động, phương tiện lưu trữ thông tin, chuyển đổi năng lượng điện, mạch điện tử, nước từ, và các ứng dụng y học. Nếu nghiên cứu chuyên sâu về khoa học từ tính, chúng ta sẽ thấy rằng nó là một lĩnh vực phong phú và đa dạng. Do đó, việc tổng hợp và diễn giải một lĩnh vực rộng lớn và đa dạng như thế trong một chương là một nhiệm vụ khó khăn.

Ở đây, chúng tôi sẽ chỉ đề cập đến những kiến thức mà chúng tôi thấy có ích và cần thiết để nghiên cứu tính chất từ của các hạt nano. Do đó, chương này không hẳn là chương trình bày về từ tính ở thang nano, mà chỉ là một chương mô tả những kiến thức cần thiết để chúng ta có thể nghiên cứu từ tính ở kích thướt nano. Trong toàn bộ chương này, chúng ta sẽ sử dụng một số nguồn kiến thức trong ba tài liệu tham khảo rất hay sau đây: sách của Cullity, hiện nay là tài liệu kinh điển về lĩnh vực này; chương 2-từ học trong sách vật lý trạng thái rắn của Kittel, và quyển sách tương đối dễ hiểu của Jiles.3 Chúng ta có thể dùng một trong ba sách đó nếu muốn tìm hiểu kỹ hơn những hiện tượng bên dưới.

these can be consulted for more detailed description of the phenomena described below.

6.2 FUNDAMENTAL CONCEPTS

6.2.1 Atomic Origins of Magnetism

It is well known that matter is electronic in nature; that is, all atoms are made of positive and negative charges (protons and electrons) that are strongly bound together via the electrostatic (Coulomb) force. This force is a consequence of the electric field, which reaches out from a charge across space to cause a force on a second charge. It is also well known that electricity and magnetism are integrally tied together as different aspects of the same thing—the electromagnetic interaction. Interestingly, there is a break in this symmetry in that, whereas electric fields occur spontaneously from electronic charges (indeed, they are each other) there are no magnetic "charges,"—in other words, magnetic monopoles do not exist. Because of this, the sole source of the magnetic field is relative motion of an electric charge and the observer. Thus magnetism is a result of moving charges. From an atomic view of matter, there are two electronic motions: the orbital motion of the electron, and the spin motion of the electron. Except for some nuclear magnetic effects, which are much smaller and which we will not discuss, these two electron motions are the source of macroscopic magnetic

phenomena in materials.

6.2.2 Magnetic Variables and Units

The magnetic field strength (or intensity) is usually represented by H. H will be reserved for fields that result solely from free currents, such as an electric current flowing in a wire. The magnetic moment per unit volume of a magnetic material is measured by M, the magnetization (or polarization). M results from the two atomic motions: the orbital and spin motion of the electron, mentioned above. These are often viewed macroscopically as equivalent or effective currents. Finally, the general case of a field due to both free and equivalent currents is described by the magnetic induction, B. These three quantities are tied together in the field equation

$$B = H + 4\pi M \quad \text{[cgs]} \tag{6.1}$$

Thus B can result from a combination of H and M. For example, an electromagnet made by winding coils of copper wire around an iron rod and then passing a current through the wire has an H from this current, an M from atomic motion of the electrons in the iron, and a total B that is the sum of these two as described by Equation (6.1).

The units of H, M, and B are fundamentally all the same, as implied by Equation (6.1), and depend on the system of units being used. There are a number of unit conventions, each with advantages and disadvantages.

There are currently three systems of units that see widespread use. Historically, workers in magnetic materials have used the cgs (centimeter, gram, second) or Gaussian system. More recently attempts have been made to change over to the SI system (in mechanics SI implies mks—meter, kilogram, second). There are two SI systems, the Kennelly and the Sommerfeld conventions, the latter slowly gaining acceptance in the magnetism community. Table 6.1 gives the units for the important magnetic quantities.

Conversion factors are:

TABLE 6.1 Magnetic units. A is ampere, cm is centimeter, m is meter, emu is electro¬magnetic unit, B is magnetic induction, H is magnetic field strength, M is magnetization of a substance per unit volume, $\mu_0 = 4\pi \times 10^{-7}$ newton/ampere^2 is the permeability of free space. In the SI-Kennelly convention the magnetization is I, the intensity of the magnetization

Quantity	cgs (emu)	SI (Sommerfeld)	SI (Kennelly)

With the information in Table 6.1, one can show:

$$1 \text{ emu} = 1 \text{ erg Oe}^{-1}$$
$$= 1 \text{ (erg cm}^3)^{1/2}$$
$$1 \text{ Oe} = 1 \text{ (erg cm}^{-3})^{1/2}$$

Also note that in the cgs system the magnetization M can also be written per gram of substance. Then one often finds the symbol a used, viz.

$$\sigma = M/\rho \quad (\text{emu g}^{-1}) \qquad (6.2)$$

$$a = M/p \quad (\text{emu g-1}) \quad (6.2)$$

where p is the mass density. Examples of magnetic fields are those of the earth, for which B ~ 0.8 G = 8 x 10 5 T, or near a pole of a common permanent magnet where B ~ 1000 G, etc. Beware, however, because usage of magnetic units is often not careful and units get mixed.

6.2.3 Magnetic Susceptibility and Permeability

Perhaps the most common magnetic experiment is to apply a magnetic field to a material and measure the magnetization induced by the field. The measure of how effective an applied field is for inducing a magnetic dipole is the susceptibility of the material, defined as

$$k = M/H \quad (6.3)$$

This susceptibility is unitless, as seen by Equation (6.1). However, it can be expressed in terms of units if M is taken as emu cm-3 for then k has units of

$$\kappa = M/H \quad (6.3)$$

TABLE 6.2 Permeabilities of some common ferromag¬netic substances.4 Permeability is a function of applied field and temperature. The values quoted here are maximum values

Substance	Permeability, ^
Transformer steel	5 x 103
Cold-rolled steel	2 x 103
High-purity iron	920
4% Si in Fe	7 x 103
78 Permalloy	105
Supermalloy	106

emu cm^3 Oe^1. For this reason, it may be thought of as the susceptibility per unit volume. Dividing by the density of the material yields the mass susceptibility,

$$\chi = \kappa/\rho \quad (\text{emu g}^{-1}\ \text{Oe}^{-1}) \tag{6.4}$$

or dividing by the mole weight yields the molar susceptibility,

$$\chi_M = \chi/\text{mole wt} \quad (\text{emu mol}^{-1}\ \text{Oe}^{-1}) \tag{6.5}$$

A quantity closely related to the susceptibility is the permeability μ defined by

$$\mu = B/H \tag{6.6}$$

The physical content of Equation (6.6), especially if it is rewritten as $B = \mu H$, is that a field H, generated by a current, when applied to a material of large permeability (e.g., μ of iron can range to thousands, see Table 6.2), is enhanced by the factor of μ to create a large field B.

From Equations (6.1), (6.3), and (6.6) it is easy to show that

$$\mu = 1 + 4\pi\kappa \tag{6.7}$$

Remember that this expression holds for the cgs system of units; similar expressions hold for other units systems.

6.3 MAGNETIC MATERIALS

For most of us the term "magnetism" conjures up visions of pieces of iron being attracted across a distance by magnets. The

layman sees only iron as magnetic; other materials are not affected by magnets. Nothing could be further from the truth, however, because all materials are affected by a magnetic field, although most only weakly so. The nature of the interaction with a magnetic field allows us to classify (roughly) magnetic phenomena into three major categories:

1. Ferromagnetism: Here the interaction is strongly attractive toward a magnetic pole. Iron, cobalt, and nickel are the classic examples of ferromagnets. A list of some ferromagnetic (and ferrimagnetic) materials is given in Table 6.3.

2. Paramagnetism: Here the interaction is weakly attractive toward a magnetic pole. A list of some paramagnetic materials is given in Table 6.4.

3. Diamagnetic: Here the interaction is weakly repulsive from a magnetic pole. The vast majority of substances are diamagnetic, including water, SiO2, wood, plastics, NaCl, CaCO3, and most organic and biological materials. Some diamagnetic materials are listed in Table 6.5.

These classifications are rough. Below we will refine the meaning of ferromag¬netic in terms of the coupling between adjacent atoms. Strictly speaking, ferri- magnets, such as magnetite (Fe3O4), are not ferromagnets but are included in the "ferromagnetic" classification above. Another

category of weakly attractive materials are antiferromagnets, which are definitely not paramagnets. Extensive tables of magnetic properties are given in reference 4.

If the material is not itself a magnet—if it has no permanent magnetic polar¬ization—then the interaction occurs because the applied field induces the material to become a magnet, that is, it induces a magnetization M into the material. Then the two magnets, one given, one induced, interact.

For a paramagnetic substance, k is small and positive. Typical values fall in the range 10-3 to 10-5 at room temperature. Because the value is positive, the induced moment has the same direction as the applied field. Figure 6.1a depicts a permanent magnet creating a field near a paramagnetic material. The field lines for B are away from the north pole of the magnet; hence, with k > 0, the induced dipole points away from the north pole of the magnet as well. The paramagnetic material has been polarized, so it is now a magnet as well. The south pole of the induced dipole is at the tail of the dipole vector, the north pole is at the head, as drawn. From elementary magnetostatics we know that a dipole tends to align with the applied field, so a nonsymmetric piece of paramagnetic material would align with its long axis parallel to the field. We also know that the
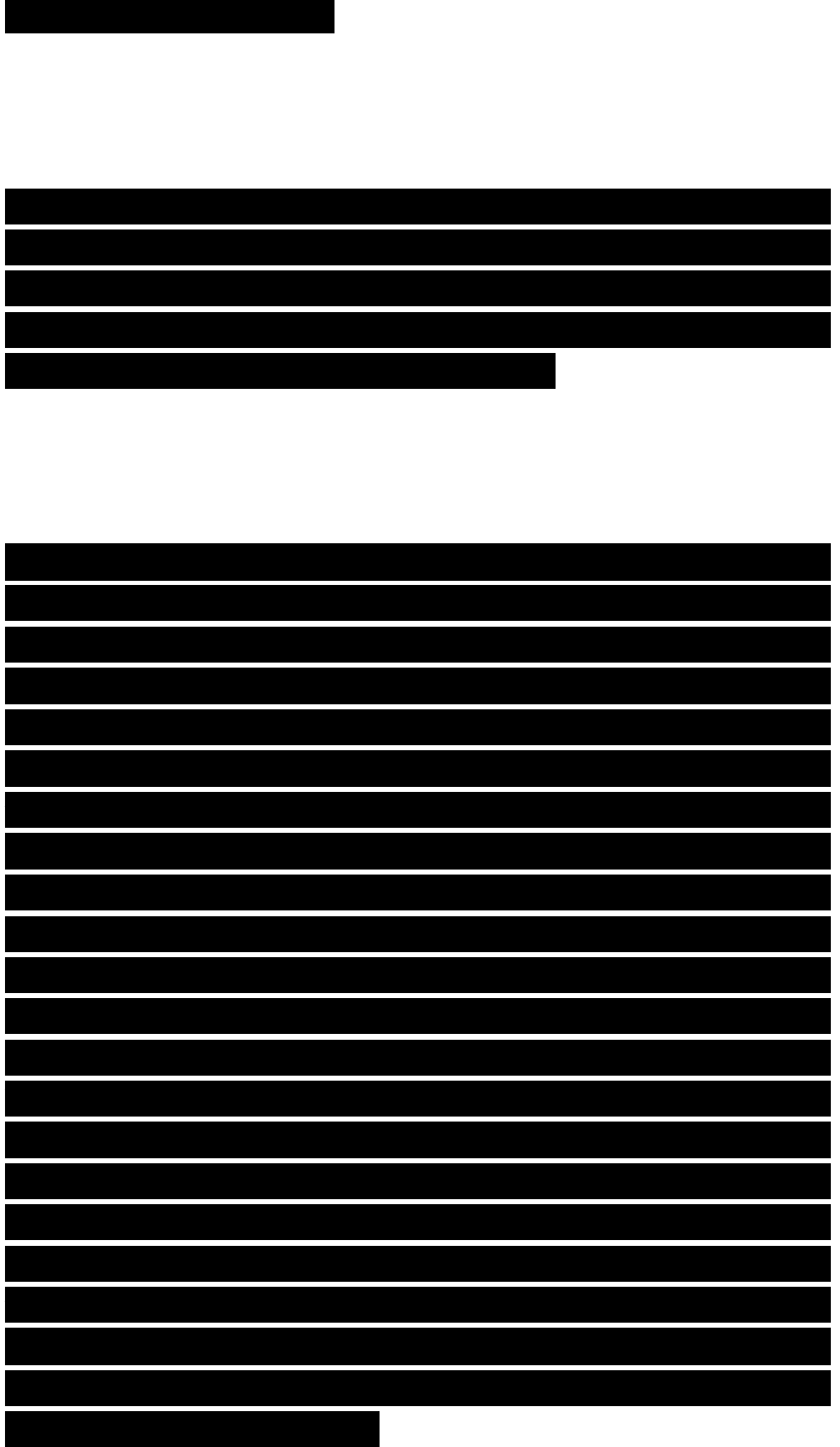
total force on a dipole in a uniform field is zero, but the field near a pole piece is far from uniform, growing weaker with distance. Thus, the attractive force between the permanent magnet's north pole and the induced magnet's south pole will dominate the repulsive interaction of the permanent and induced north poles for an overall attraction. This scheme holds true for a ferromagnetic material since $k > 0$ again. The difference, and it is major, is that ferromagnetic susceptibilities are typically orders of magnitude greater than para-magnetic ones, so that the force is much greater as well.

A diamagnetic material has $k < 0$, with typical values on the order of 10^5 to 10^{-6}. Thus, when such a material experiences an applied field, the induced moment is small and opposite to the field, as depicted in Figure 6.1b. The induced dipole

TABLE 6.3 Ferromagnetic and ferrimagnetic materials

Saturation Magnetization Ms, in emu cm-3 (or emug-1)
Curie Temperature

Bohr Magnetons

Substance Temperature   0 K per Formula Unit (°C) (K)
Compiled from references 2, 3, and 4.

would try to rotate from this anti-aligned state to an aligned state, but the dipole is not connected to

the material, rather its direction is determined by the applied field. If the object is not symmetric, e.g., a long cylinder, the cylinder will align perpendicular to the field so that the total induced moment, which would lie across the axis of the cylinder still antiparallel to H, will be minimized. In this anti-aligned state with the gradient in the applied field, we see that the repulsion of the nearby north poles dominates the attraction of the permanent magnet's north pole with the distant induced south pole, to yield an overall repulsion.

Figure 6.2 shows the magnetic state of the elements at room temperature. We see that most metals are paramagnetic. Iron, cobalt, and nickel, and below 16°C gadolinium, are ferromagnetic. Most nonmetals are diamagnetic.

TABLE 6.4 Magnetic molar susceptibility of some paramagnetic substances at room temperature

6.3.1 Diamagnetism

Diamagnetism results from a fundamental principle of electromagnetism, known as Lenz's law, which states that when a conducting loop is acted upon by an applied magnetic field a current is induced in the loop that counteracts the change in the field.

From a semiclassical, atomic point of view, the electron orbits are resistanceless, so the induced current remains after the field has

been applied and is constant. The conduction electrons of a metal, the Fermi sea, also respond in a resistanceless manner. This is also true for superconductors, which are perfectly diamagnetic (i.e., k =-1) and hence show total exclusion of the applied field.

The diamagnetism of atoms, ions, and molecules can be modeled as if the orbits of the electrons were current loops. The induced moment is proportional to the current times the area of the loop. Current will depend on the passage of charge, which is the number of electrons times the charge on the electron, e, and on the frequency of the orbital motion, which also depends on the charge e. Thus one might expect a susceptibility with functionality going as Ze2{r2), where r is the orbital radius. Indeed, the simple Langevin theory of diamagnetism predicts

$$\kappa = -\frac{NZe^2}{mc^2}\langle r^2 \rangle \qquad (6.8)$$

In Equation (6.8), N is the number of atoms per unit volume, m is the electron mass, and c is the speed of light.

TABLE 6.5 Magnetic molar susceptibility of some diamagnetic substances

Compiled from reference 4.

Equation (6.8) tells us that large atoms (high Z and large <r2)) have large diamagnetic susceptibilities. It also shows no temperature dependence, a key para¬meter for other types of magnetism. Table 6.5 gives the diamagnetic susceptibility for a few selected materials.

6.3.2 Paramagnetism

Paramagnetism occurs when the atomic, ionic, or molecular constituents have a nonzero magnetic moment. Then an applied field can align these moments to create a positive susceptibility. The diamagnetic response is still present, but the atomic moments have a much greater magnitude than the induced diamagnetic moments. The source of atomic scale magnetic moments is unbalanced angular momentum of

FIGURE 6.1 A magnetic field applied to an elongated material. (a) When k > 0, the induced dipole is in the same direction as the applied field and the net force is attractive. (b) When k < 0 (diamagnetic) the induced dipole is opposite to the applied field and to minimize this unfavorable antiparallel alignment the material rotates its axis perpendicular to the field. The net force is repulsive.

the electrons, either orbital or spin. Both angular momenta yield a magnetic moment given by

$M = g M_B J$

$$\mu = g\mu_{\mathrm{B}} J \qquad\qquad (6.9)$$

In Equation (6.9), g is the so-called g factor. For a free electron, g ~ 2.00. The Bohr magneton M_B is given by

FIGURE 6.2 Magnetic state of the elements at room temperature (T = 20°C). *Gadolinium becomes ferromagnetic at 16°C.

where $h = h/2\pi$ and h is the Planck constant. This is the

fundamental unit of magnetism. Note its magnitude: a macroscopic quantity of Bohr magnetons, say 1023, would yield a healthy magnet; a fact which fortunately does transpire. Finally, Equation (6.9) contains the angular momentum quantum number J, which is of order unity. For a free electron the angular momentum is purely spin and so J = S = 1, hence

p = SPB S = Pb

Nonzero magnetic moments leading to paramagnets can occur in many materials. Spin moments can result in atoms or molecules with an odd number of electrons, in transition metals with partially filled ^-shells, and in rare earths with partially filled f -shells. Orbital moments also contribute in the rare earths (hence their large moments), but are quenched to zero in the transition metals. Many other metals are paramagnetic due to the electrons within kT (the thermal energy) of the top of the conduction band (Pauli paramagnetism). There are a few cases of compounds with an even number of electrons that are paramagnetic, such as molecular oxygen.

Even a very small applied field would readily align all the atomic moments and create a significant polarization if it were not for the randomizing effect of thermal motion. Indeed, the energy of magnetic moment alignment in an applied field and the thermal energy, which causes randomization, are the primary

$$\mu = g\mu_{\mathrm{B}} S = \mu_{\mathrm{B}} \qquad\qquad (6.11)$$

actors in the phenomena of paramagnetism and ferromagnetism. The simplest model that uses this competition is the Langevin model of paramagnetism, which gives us our first intuition into the importance of temperature for magnetic properties.

6.3.2.1 The Langevin Model of Paramagnetism

We consider N atoms each with a magnetic moment of p. In an applied field the moment tends to align with the field and the energy of interaction is

$$U = -\vec{\mu} \cdot \vec{H}$$
$$= -\mu H \cos\theta \qquad (6.12)$$

where θ is the angle between p and H. Note that Equation (6.12) assumes that the moment can point in any direction relative to H. This is only true for non-quantum- mechanical moments. While such moments do exist (for example, see the descrip¬tion of superparamagnetism below), this is definitely not true for atomic moments, so we proceed with caution.

The total moment of the macroscopic body will be proportional to p, the number of atoms (per unit volume) N, and the degree of alignment. The alignment is measured by $\cos\theta$, and since there are many moments, we need the average of $\cos\theta$. Thus

$$M = N\mu\langle\cos\theta\rangle \qquad (6.13)$$

The average alignment $\langle\cos\theta\rangle$ can be obtained from the probability of having a given cos

6. In a system in thermal equilibrium at temperature T, the probability is given by the Boltzmann distribution

$$p(U) = e^{-U/kT} \tag{6.14}$$

In Equation (6.14) k is Boltzmann's constant, $k = 1.38 \times 10^{-16}$ erg K^{-1}. Then

$$\langle \cos\theta \rangle = \frac{\int \cos\theta \, e^{-U/kT} \, d\Omega}{\int e^{-U/kT} \, d\Omega} \tag{6.15}$$

The integration is over all solid angles, $d\Omega$. The integration is straightforward and one obtains

$$M = N\mu L(x) \tag{6.16a}$$
$$L(x) = \coth x - x^{-1} \tag{6.16b}$$
$$x = \mu H/kT \tag{6.16c}$$

Equation (6.16b) is the Langevin function. In Equation (6.16c) the parameter x is the ratio of magnetic alignment energy to thermal randomizing energy, and hence gives emphasis to the competition between these two. To gain a feel for the Langevin result we look at its properties at small and large x. At small x,

$$L(x) \simeq x/3 \tag{6.17}$$

Hence the magnetization is

$$M \simeq \frac{N\mu^2 H}{3kT} = \frac{C}{T} H \tag{6.18}$$

This result with its inverse temperature dependence is known as the Curie law, and C is the Curie constant given by

$$C = \frac{N\mu^2}{3k} \tag{6.19}$$

Equation (6.18) applies when kT ^ pH. For example, if p = pB = 0.927 x 10-20 erg Oe-1, and if T ~ 300 K (roughly room temperature), x = 1 when H = 1.2 x 105 Oe = 12 T. Thus, it takes huge fields to align paramagnets signifi¬cantly at normal temperatures. On the other hand, if T = 4 K, then a relatively modest field of H = 1.6 x 103 Oe = 0.16T will give x = 1 and some alignment.

At large x, L(x) ^ 1, and all the moments are aligned. This is called the saturation magnetization,

$$M_s = N\mu \qquad (6.20)$$

Ms = N p   (6.20)

In Figure 6.3 L(x) is plotted against x.

6.3.2.2   Quantum Effects

An atomic scale angular momentum will be controlled by quantum mechanics and hence only selected, discrete values of moment orien¬tation relative to the applied field will be allowed. For an angular momentum J there will be 2J + 1 possible orientations of the moment as described by the azimuthal quantum number mJ = J, J — 1, ..., — J. After this modification, the physics of alignment in an applied field at finite temperature is the same, viz., the competition between field alignment and thermal randomization. The Boltzmann distribution is still used to calculate the average orientation. The general result is

$$M = NgJ\mu_{\mathrm{B}}B_J(x) \qquad (6.21a)$$

M = NgJ ^B BJ (x)(6.21a)

Where

$$B_J(x) = \frac{2J+1}{2J}\coth\left(\frac{(2J+1)x}{2J}\right) - \frac{1}{2J}\coth\left(\frac{x}{2J}\right) \qquad (6.21b)$$

FIGURE 6.3 The Langevin function for classical paramagnetism.1 and

$$x = gJ\mu_B H/kT \qquad (6.21c)$$

The function $B_J(x)$ is called the Brillouin function. For $x \ll 1$, a typical situation near room temperature, one can show that Equations (6.21) yield

$$M \simeq \frac{NJ(J+1)g^2\mu_B^2}{3kT} H \qquad (6.22)$$

The Curie law, $M = C/T$, is regained. The effective magnetic moment resides in the Curie constant C and is equal to $\mu_{eff} = g\sqrt{J(J+1)}\mu_B$ by comparison with Equations (6.18) and (6.22). The Brillouin function has two significant limits with J. When $J = \frac{1}{2}$, there are only two states and it is easy to show that

$$M = N\mu\tanh x \qquad (6.23)$$

results. When $J \to \infty$, the Brillouin function becomes the Langevin function (Equation 6.16b). Figure 6.4 shows a plot of M versus $x = gJ\mu_B H/kT$ for the Brillouin result (Equations 6.21), for various J, and we see that the shape evolves somewhat as we go from the simplest quantum mechanical limit of two states ($J = \frac{1}{2}$) to the classical, Langevin

limit $(J \wedge ro)$.

FIGURE 6.4 The Brillouin function for quantum paramagnetism for various values of J.

6.3.2.3 Experimental Implications From an experimentalist's point of view, the theory above implies that magnetization data for a paramagnet fall on a universal curve if plotted as a function of H/T. Conversely, any data that show universality with plotting M versus H/T imply the system could be paramagnetic.

Avery useful technique is the Curie plot, in which inverse susceptibility is plotted versus T. By the Curie law (Equation 6.18), $k = C/T$. Thus, a straight line is obtained if the system is paramagnetic. Furthermore, the inverse of the slope of k_1 versus T yields C, the Curie constant, from which the magnetic moment of the atomic entity can be determined from Equations (6.19) or (6.22). Figure 6.5 shows a schematic of the behavior of both k and k_1 versus T for a paramagnet.

6.3.3 Ferromagnetism

6.3.3.1 The Curie-Weiss Law The Curie law for paramagnetism (Equation 6.15) has been found to hold for many materials. However, many other materials display a somewhat modified behavior described by

(6-24)

$$\kappa = \frac{C}{T - \theta} \tag{6.24}$$

FIGURE 6.5 The behavior of the susceptibility k and its inverse as a function of temperature for para-, ferro-, and antiferromagnetic materials.[1] where 6 is a critical temperature that can be either positive or negative. This modification is called the Curie-Weiss law. Equation (6.24) is a remarkable result because it diverges at 6, which is a finite temperature when 6 is positive. Since K = M/H, this means that a net magnetization (M = 0) can be achieved even if the applied magnetic field is zero. We would say the system has a spontaneous magnetization.

To explain this empirical result, Weiss proposed that the atomic moments were interacting with each other magnetically. To model this interaction he assumed that the net interaction on a given moment is an effective magnetic field, a mean field, due to all the other moments. It is reasonable to propose that this effective field is proportional to the magnetization of the material, hence

$$H_E = \alpha M \tag{6.25}$$

He = aM   (6.25)

Then the total field experienced by any given moment is

Htot = H + aM   (6.26)

$$H_{tot} = H + \alpha M \tag{6.26}$$

It is with this total field that the thermal energy "fights." Thus, the Curie law still holds but with the

modification

$$\kappa' = \frac{M}{H_{tot}} = \frac{C}{T} \tag{6.27}$$

Substitution of Equation (6.26) into (6.27) yields

$$\kappa = \frac{M}{H} = \frac{C}{T - \alpha C} \tag{6.28}$$

With this, we regain the Curie-Weiss law of Equation (6.24) with $\theta = \alpha C$.

A more careful look at the data near the divergence or critical temperature $T_c = \theta$ for materials following the Curie-Weiss law (e.g., ferromagnets) reveals that the susceptibility is better described by

$$\kappa \propto (T - T_c)^{-\gamma} \tag{6.29}$$

where $\gamma \sim 1.3$, inconsistent with the mean field prediction. Furthermore, using $T_c = \alpha C$ leads to unrealistically large values of H_e; for example, for iron $T_c \sim 1000$ K and then $H_e \sim 10^7 oe$! Thus, the mean field theory has serious problems. More accurate theories consider only nearest-neighbor interactions for the atomic moments and the interactions are not magnetic, but rather due to what is called an exchange interaction, which is quantum mechanical in origin. The Weiss theory works semiquantitatively because the basic concept of an interaction between atomic moments is correct.

Weiss, in 1906, realized that the spontaneous magnetization that occurs below T_c could be used to explain ferromagnetism. Then we

view a ferromagnet as a material that is self-starting. However, there must be more because if there is only a molecular field, every piece of iron would have a significant dipole moment, and this is obviously not the case. To contend with this, Weiss proposed that ferromagnetic materials can partition themselves into domains. Each domain is saturated by its molecular field, but the domains align in a manner that leaves a net zero magneti¬zation. We will discuss domains below.

A theory for the temperature dependence of the spontaneous magnetization can be developed by simply substituting $H = He = aM$ into the equations for the paramagnetic magnetization. The most general approach would use the Brillouin function. We write (6.30)

$$M = M_0 B_J\left(\frac{gJ\mu_B \alpha M}{kT}\right) \qquad (6.30)$$

Such an equation must be solved numerically. One finds for $T > 6 = aC$, $M = 0$, but for $T < 6$ a temperature dependent spontaneous magnetization occurs, Ms(T), which is the solution to Equation (6.30). Recall from Equation (6.28) that $6 = aC$. Then if we define the reduced variables $m = Ms(t)/M0$ and $t = T/6$, we can write

m = BJ (m/t)

$$m = B_J(m/t) \qquad (6.31)$$

Equation (6.31) shows that for a given J all data for a variety of ferromagnetic materials would lie together if plotted with reduced variables. This is a "law of corresponding states," very similar to the same law found for

fluids near critical points. Figure 6.6 shows the numerical solutions to (6.30) and some data for iron, cobalt, and nickel.

Expansion of (6.30) at small m shows that m ~(t — 1)1/2. In fact experiment gives m ~(t — 1)fi with the critical exponential — 0.35. As with the susceptibility exponent above, this discrepancy is due to the mean field nature of the Curie-Weiss theory. Theories involving only local, nearest-neighbor interactions are successful in predicting the correct exponents.

When Ms(T) ^ M0 at low temperature, Equation (6.30) again fails to predict the proper temperature dependence. In this regime, when all the spins are nearly aligned, the thermal energy can excite spin waves, quantized excitations of the atomic spins tipped slightly away from the perfectly aligned state, as drawn in Figure 6.7. Then the magnetization follows Bloch's law:

M(T)=M0(1 — BTb)

$$M(T) = M_0(1 - BT^b) \qquad\qquad (6.32)$$

B is called the Bloch constant and the Bloch exponent is b = d/2, where d is the spatial dimension, typically d = 3. Figure 6.8 shows an example of Bloch's law for both bulk and nanoscale materials.5

6.3.3.2 Origins of Ferromagnetism

Weiss molecular field theory is very successful in semiquantitatively describing the onset and behavior of ferromagnet-

FIGURE 6.6 Saturation magnetization versus temperature, both as scaled variables. Lines are predictions of the mean field theory for ferromagnetism using the quantum Brillouin function with three different /-values. Points are data for iron, cobalt, and nickel.[1]

ism. It predicts spontaneous magnetization (i.e., does not need an applied field) below a critical temperature, called the Curie temperature, and paramagnetic beha¬vior (Curie-Weiss) above. We have seen, however, that it misses in the details of the temperature dependence, and the magnitude of the molecular field seems unrea¬sonably high. This latter aspect implies that the origin of the interatomic coupling is unknown. The true physical origin of the coupling was elucidated by Heisenberg in 1928, following the Heitler-London treatment of the hydrogen molecule. Quantum mechanics provides for an exchange interaction, as it is now called, between two atoms based on symmetry, the Pauli exclusion principle, and the coulombic inter¬action. A two-electron system, one from each atom, can have one of either two spin configurations: parallel or antiparallel signs. If the atoms are brought near to each other, the electron wavefunctions will overlap, and if they are from the same atomic quantum state, the Pauli exclusion principle will
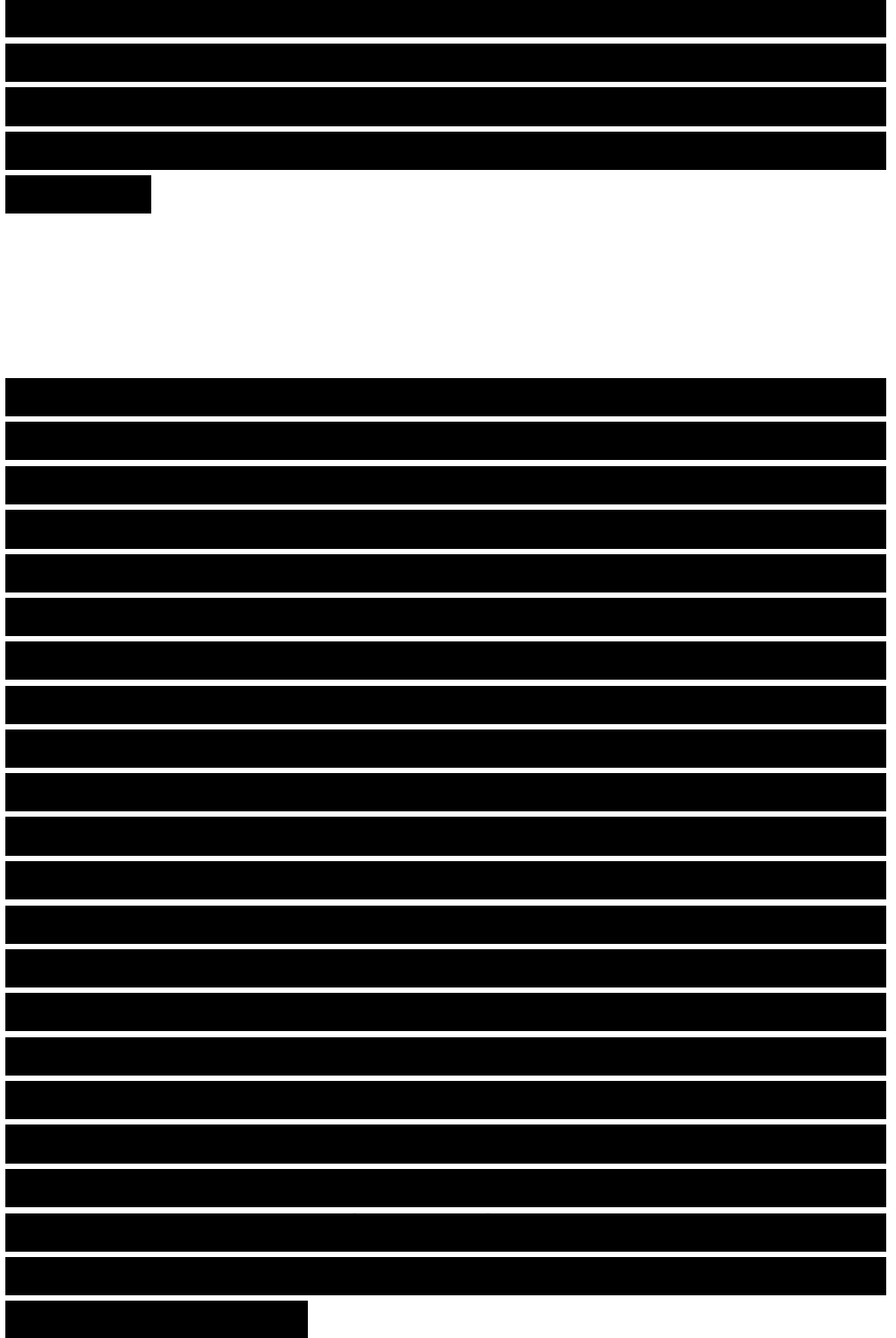
enhance the probability for the electron wavefunction to overlap if the spins are antiparallel and tend to keep them apart when the spins are parallel, for then all four quantum numbers (three atomic, one spin) would be the same. This, combined with the coulombic interaction, means that parallel and antiparallel spin configurations will have different energies.

FIGURE 6.7 Schematic drawing of spin wave. Kittel, Introduction to Solid State Physics, 7E, Copyright© 1995 John Wiley & Sons, Inc. Reprinted by permission of John Wiley & Sons, Inc.

Heisenberg showed that these effects lead to an exchange energy given by
$$\hat{} _{ex} = 2 J_{ex} S_i \cdot S_j$$

$$E_{ex} = -2 J_{ex} \vec{S}_i \cdot \vec{S}_j \qquad (6.33)$$

between neighboring spins, S_i and S_j. J_{ex} is called the exchange integral. If J_{ex} is positive, the lower energy configuration is that of parallel spins, and hence parallel magnetic moments as required for ferromagnetism. If J_{ex} is negative, the antiparallel configuration results, a situation that leads to antiferromagnetism. 100 n k)

FIGURE 6.8 Saturation magnetization depression relative to its value at 0K versus temperature for different size iron

crystallites in a matrix of MgF_2. By Bloch's law (Equation 6.32), this log-log plot should have a slope of b. Reprinted with permission from D. Zhang et al, Phys. Rev. B, 1998, 58, 1467, American Physical Society.

Interestingly, the most common situation is $J_{ex} < 0$, antiparallel coupling (this happens in the covalent bond of the hydrogen molecule). However, fortunately (for much of our technology!) $J_{ex} > 0$ also occurs in rare cases and ferromagnets can result. Slater found empirically that a correlation exists between the ratio of the interatomic distance $2r_a$ to the radius of the incompletely filled d shell r_d of some transition metal elements and the sign of the exchange integral. Subsequently, Bethe was able to use quantum mechanics to explain this observation. The result is called the Bethe-Slater curve and is shown in Figure 6.9. Unbalanced spins in the d subshell of iron, cobalt, and nickel are the source of their magnetism. The Bethe- Slater curve correctly differentiates iron, cobalt, and nickel as having positive J_{ex} and hence being ferromagnetic. Moreover, the magnitude of J_{ex} is in the order of Ni-Fe- Co, which is also the order of their Curie temperatures. It also correctly predicts the antiferromagnetism of chromium and manganese, and correctly correlates their antiferromagnetic ordering temperatures. It also implies that if one could
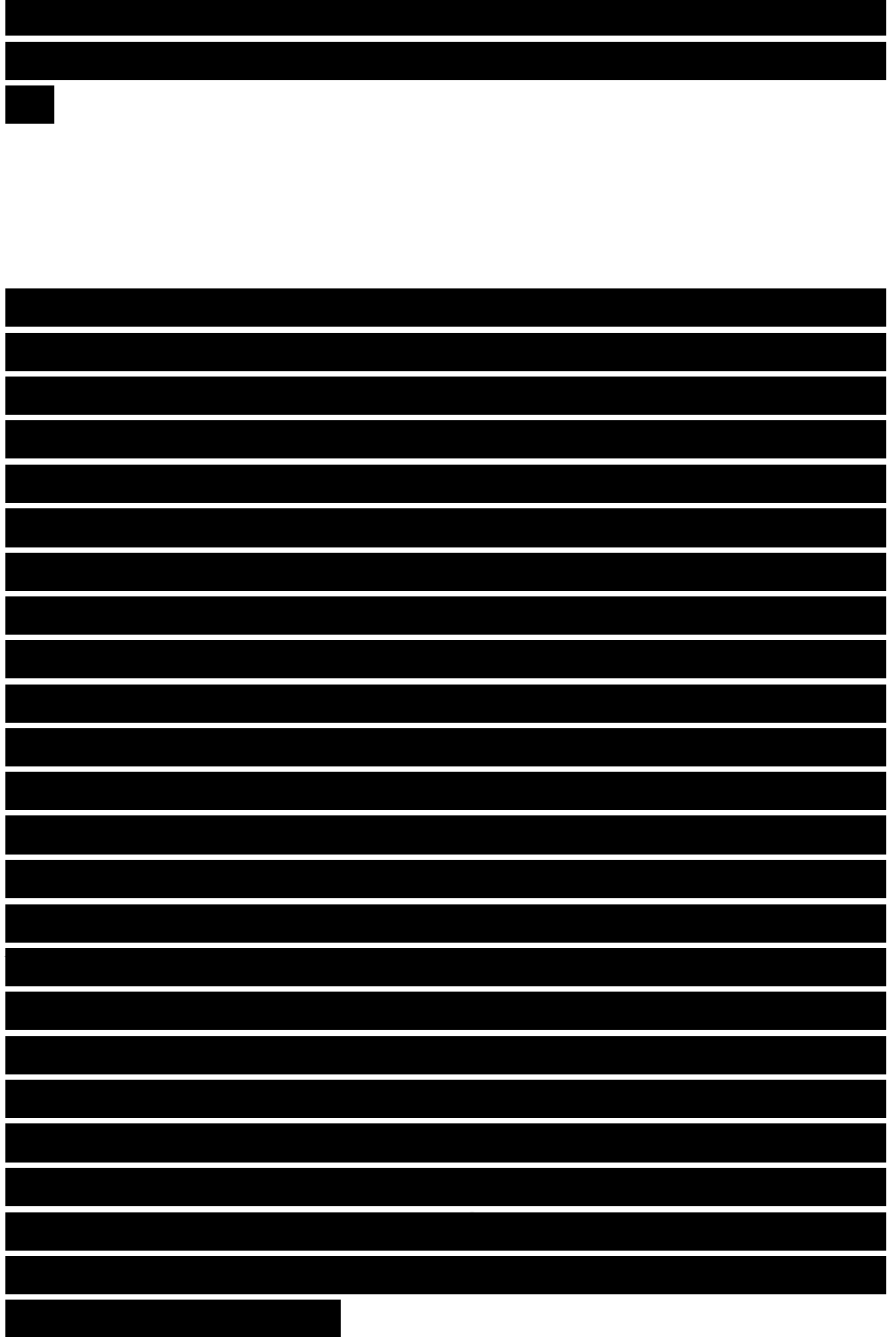
somehow change the atomic spacings, magnetic properties would change. Thus, alloys such as MnBi are ferromagnetic because the manganese atoms are farther apart in the alloy than in the pure metal and hence $2r_a/r_d$ has increased, taking manganese into the $/ex > 0$ regime of the Bethe-Slater curve. These successes have occurred despite criticism of the Bethe calculation.

6.3.3.3 Band Theory

We next contend with the problem of identifying the source of magnetic moments in the first row of transition metals, most notably iron, cobalt, and nickel. A first guess would be to look at the unbalanced spins in the 3d shell that is being filled as one progresses across the row from scandium to zinc. At scandium the first electron is added to the 3d shell "below" the 4s shell that was filled beyond argon with potassium and calcium. After scandium, as electrons are added, they all go in (by Hund's rule) with the same spin, say spin-up, until at chromium and manganese five spin-up electrons reside in the 3d shell (chromium has a $3d^54s^1$ configuration, manganese has $3d^54s^2$). This excess spin yields a spin magnetic moment of $5\mu_B$ for these atoms. Progressing now to higher atomic number, the spin-down half of the 3d shell fills, compensating the already filled spin-up shell; thus iron has a $4s^23d^6$ configuration and a net spin of 4. And, indeed, these magnetic

FIGURE 6.9 The Bethe-Slater curve. 2ra/rd is the atomic separation divided by the radius of the atomic d-shell; /ex is the exchange integral and positive values yield ferromagnetic coupling, negative values yield antiferromagnetic coupling.

moments are observed, with various perturbations, in insulating compounds of the transition metals. Much of this changes when the atoms are brought together to form a solid metal. Most notably, the discrete atomic energy levels broaden greatly to form electronic bands. In the 3d transition metals, the outermost 4s state broadens the most, followed by the 3d level, which also broadens significantly. The shells closer to the nucleus do not overlap significantly, hence neither do they broaden. Figure 6.10 gives a sche¬matic picture of the 4s and 3d bands and significant overlap in energy (plotted on the vertical axis) is seen. The density of states per energy interval is plotted horizontally, to the right for the 4s bands and to the left for the 3d band. The total area of each band in this diagram is the total number of possible states per atom: two for the 4s and 10 for the 3d, a remnant of the atomic configuration. The extent to which these bands are filled by electrons depends on the number of 3d plus 4s electrons in the atom. The level to which the
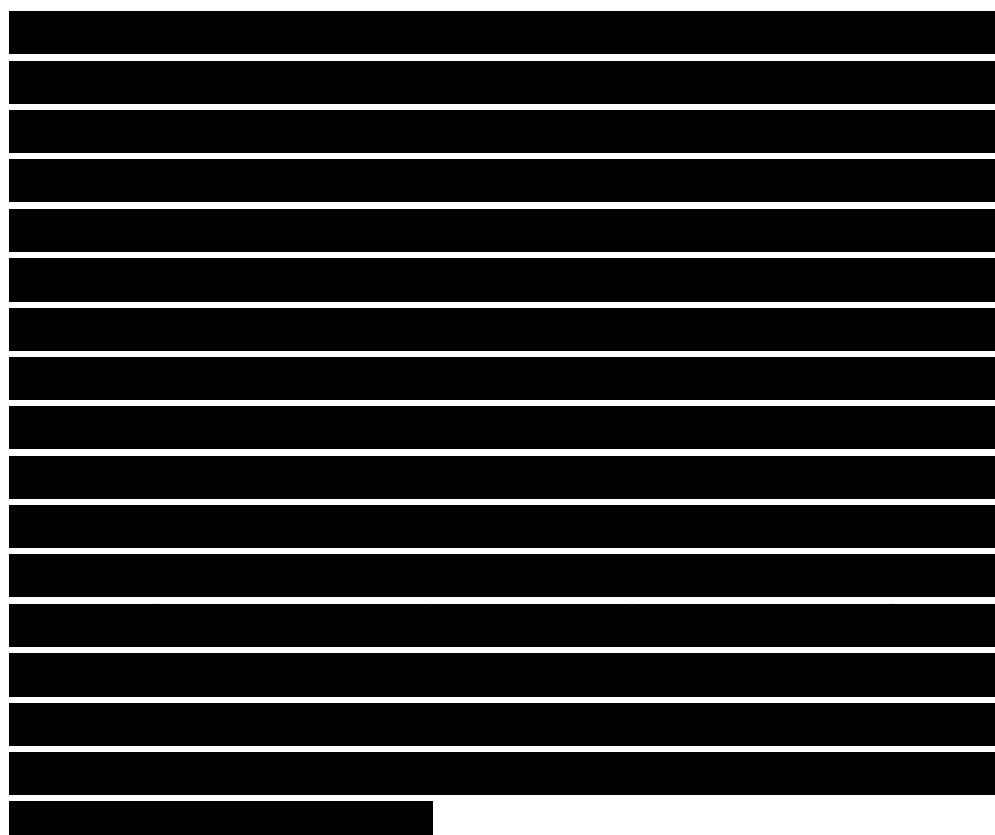
bands are filled is the Fermi level, and such levels are shown for the atoms manganese through zinc.

Consider nickel, which has eight 3d electrons and two 4s electrons in the atomic state. In the metal these ten electrons fill up and mix in both the 3d and 4s bands to the same Fermi level. It is known from the magnetic properties of nickel that the 3d is filled to the 9.4 electron level and the 4s band is filled to the 0.6 level.

It is at this point that the exchange energy comes into play. We have discussed how exchange creates the coupling of magnetic moments necessary for spontaneous magnetization. But it has another related, and very important, role which is to create a spin imbalance in the band. Since parallel spins interact with a different energy

Density of states ▶

FIGURE 6.10 Schematic of the 3d and 4s electron bands of the first-row transition elements. Fermi levels are marked for various elements.

from antiparallel spins, the 3d band splits into spin-up and spin-down with different energies. Thus the nearly filled (9.4) 3d band of nickel is in fact a completely filled spin-up band of five electrons and a partially filled spin-down band of 4.4 electrons. The net result is 0.6 unbalanced spin, from which a net magnetic moment of $0.6 \mu_B$ results.

We can now extend this picture to other elements in the 3d row of

the periodic table. Moving left to cobalt removes one 3d electron per atom, so if nickel is short 0.6 electrons, cobalt should be short 1.6. Likewise, iron and manganese should be short 2.6 and 3.6, respectively, and in all cases their spins are unbalanced. Moving to the right to copper adds an electron and overfills the 3d band by 0.4 electrons. Thus, copper is not ferromagnetic because the 3d band is full, hence there is no spin imbalance. The magnetic moments thus should be short by values times μ_B, the Bohr magneton. This linear prediction is plotted in Figure 6.11 along with the measured moments; reasonable agreement is seen, thus substantiating the band theory.

Slater used these ideas to explain the ferromagnetism of simple alloys. For example, what is the magnetic moment of an equimolar mixture of nickel and copper? Since nickel has a 3d band underfilled by 0.6 electrons and copper has a 3d band overfilled by 0.4 electrons, this equimolar mixture should have a 3d band filling of $(0.5)(+0.6) + (0.5)(-0.4) = +0.1$ and hence be ferromagnetic with a moment of 0.1 μ_B per atom. Similar arguments can be made with success for other combinations of 3d elements. This theory is useful not only for alloys but for the general concept that if one can manipulate the d-band of a transition metal, one can manipulate its magnetism.
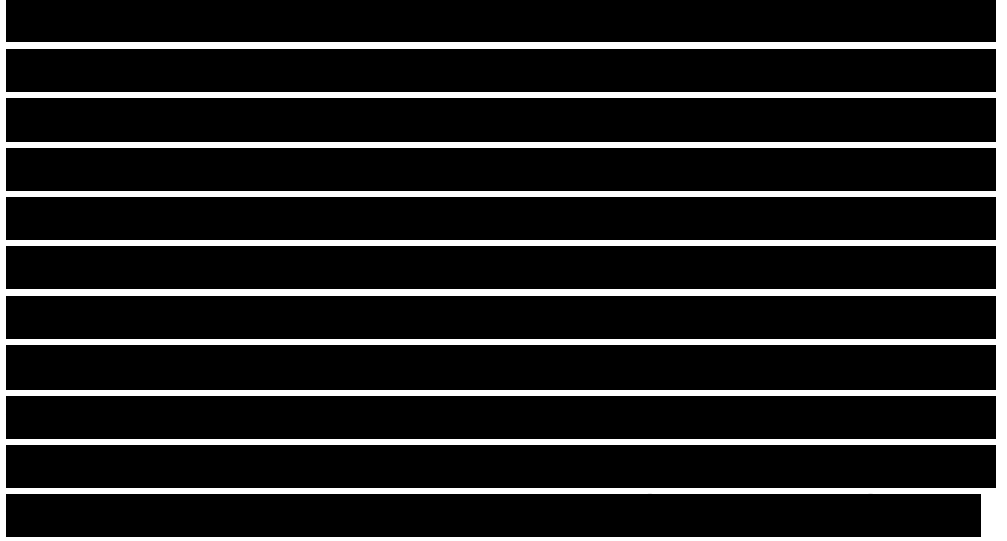
FIGURE 6.11 Band theory prediction (line) for the number of Bohr magnetons per atom for a number of the 3d transition metals. A value less than or equal to zero implies the metal is not ferromagnetic. Circles are data.

6,3,3,4 Antiferromagnetism
In an antiferromagnet, exchange coupling exists between neighboring moments that causes the moments to align in an antiparallel fashion: the exact opposite of a ferromagnet. Thus, in terms of the Heisenburg hamiltonian of Equation (6.33), the exchange integral Jex is negative. This anti¬parallel alignment causes the system to have a small, positive susceptibility, because an applied field tends to align the spins and this induced alignment is larger than the diamagnetism of the electron orbitals. Similar to ferromagnets, the exchange energy can be defeated at high temperature and then the system becomes para¬magnetic.

The behavior of the antiferromagnetic susceptibility is depicted in Figure 6.5 and in more detail in Figure 6.12. For temperatures greater than a critical temperature, the susceptibility follows a paramagnetic Curie-Weiss law with a negative 6. Thus, ferromagnets and antiferromagnets are akin at high T following Curie-Weiss, differing only in the sign of 6.
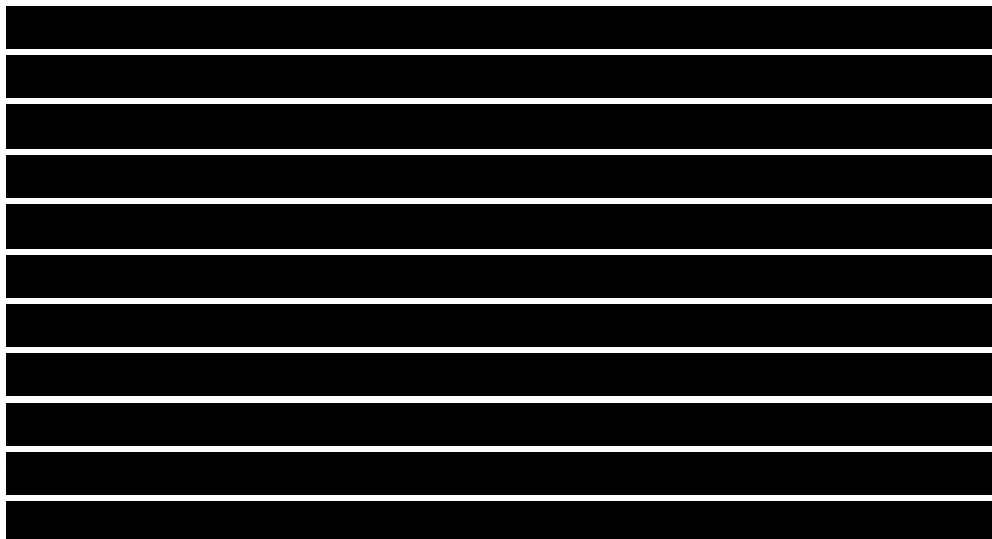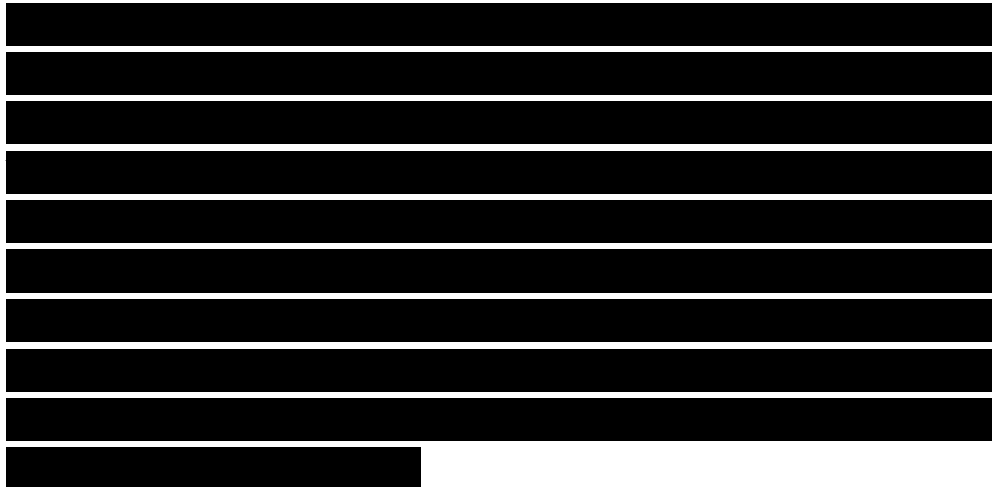
This kinship and difference are a direct consequence of the same Heisenburg hamiltonian but differing signs in the exchange integral. Below the critical temperature TN, the Neel temperature, the system orders. Thereafter, the susceptibility decreases with decreasing temperature because the tendency for antiparallel alignment increases. Many antiferromagnetic systems are known, usually ionic compounds such as metallic oxides, sulfides, chlorides, and so on. Both chromium and manganese are antiferromagnetic, although their suscept¬ibilities do not obey the Curie-Weiss law. See Table 6.6 for other examples.

A microscopic view of an antiferromagnet is depicted in Figure 6.13. There we see two sublattices, usually called A and B. A molecular field theory for anti¬ferromagnetism incorporating only the antiparallel interaction of the A and B

TABLE 6.6 Antiferromagnetic substances

Substance Paramagnetic Ion Lattice" Transition Temperature TN (K) Curie-Weiss

FIGURE 6.13 Schematic depiction of spin arrangements in a ferromagnet, an antiferro¬magnet, and a ferrimagnet.

sublattices predicts that 6/TN = 1. Table 6.6 shows that this is rarely the case and the reason is due to interactions within each

sublattice.

The exchange interaction in antiferromagnetic ionic solids occurs indirectly via a mechanism called superexchange. The nearest neighbors to the metallic ions, which carry the magnetic moment, are anions such as 02~, S2~ and Cl. Thus, for two metallic ions to communicate their spin states to each other they must work through an anion. This occurs by spin polarizing the outer electron orbitals of the anion so the spin information can be conveyed.

Antiferromagnets can be quite complex and do not always display the canonical behavior of Figure 6.12. This is especially true for nonionic systems such as metallic chromium and manganese and alloy systems. In such cases neutron diffraction, which can sense spin alignments at the atomic level, is necessary to positively identify an antiferromagnet.

6.3.3.S   Ferrimagnetism

Ferrimagnets are similar to antiferromagnets in that two sublattices exist that couple through a superexchange mechanism to create an antiparallel alignment. However, unlike an antiferromagnet, the magnetic moments on the ions of the sublattices are not equal and hence they do not cancel; rather, a finite difference remains to leave a net magnetization. This spontaneous magneti¬zation is defeated by the thermal energy above a critical temperature

called the Curie temperature, and then the system is paramagnetic. The behavior of the susceptibility of a ferrimagnetic is depicted in Figure 6.14. At high temperatures Curie-Weiss behavior is seen with k_1 linear with T. As for an antiferromagnet, this linear behavior extrapolates to a negative 6. Near the Curie temperature, k_1 versus T is curved.

A microscopic view of a ferrimagnet is depicted in Figure 6.13.

A large number of ferrimagnets are known; a major class of which are the ferrites. There are two types of ferrites: cubic and hexagonal. Cubic ferrites have the general

FIGURE 6.14 Curie plot, inverse susceptibility versus temperature, for a ferrimagnet (solid line). Tc is the Curie temperature below which the system has a spontaneous magnetization. Dashed line is the Curie-Weiss law.

formula $MOFe_2O_3$, where M is a divalent metal cation such as Mn, Ni, Fe, Co, and Mg. One of these is the oldest known magnetic material, magnetite or loadstone which is $FeOFe_2O_3$ or equivalently Fe_3O_4. Hexagonal ferrites have the general formula $MO_6Fe_2O_3$. Perhaps the best-known example is barium ferrite, $BaO_6Fe_2O_3$.

As the general formulas imply, the ferrites have two sublattices.
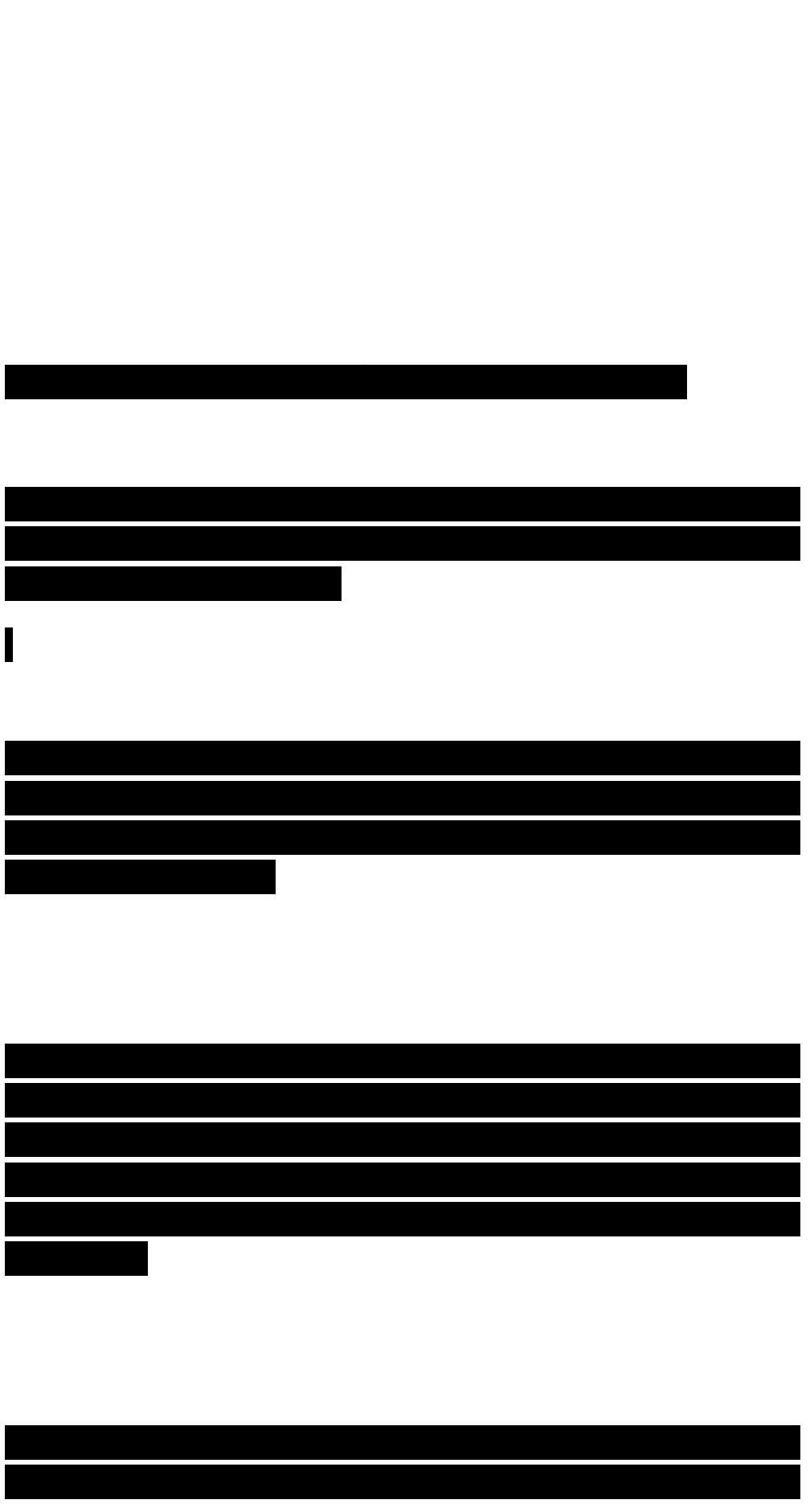
In the cubic ferrites the metallic ions in the A sublattice are tetrahedrally coordinated by oxygen atoms, whereas the ions in the B sublattice are octahedrally coordinated. Such a structure is called a spinel, and they are quite complex because there are 56 atoms in the unit cell. Moreover, the ions in the two sublattices can interchange depending on synthesis conditions or thermal treatment.

Ferrimagnets are technologically useful because they have a spontaneous magnetization and they are insulators as well.

Other classes of ferrimagnetic materials include the garnets and some alloys.

6.4 MAGNETIC PHENOMENA IN FERROMAGNETIC MATERIALS

6.4.1 Magnetic Anisotropy

In many situations the susceptibility of a material will depend on the direction in which it is measured. Such a situation is called magnetic anisotropy. When magnetic anisotropy exists, the total magnetization of a ferromagnet Ms will prefer to lie along a special direction called the easy axis. The energy associated with this alignment is called the anisotropy energy and in its lowest order form is given by

$$E_a = K \sin^2 \theta \qquad (6.34)$$

where e is the angle between Ms and the easy axis. K is the

anisotropy constant.

There are several causes from which anisotropy may occur, including those induced by stress and prior mechanical handling of the material. Here we will discuss two important and common sources of anisotropy, which are magneto- crystalline anisotropy and shape anisotropy.

6.4.1.1 Magnetocrystalline Anisotropy Only magnetocrystalline anisotropy, or simply crystal anisotropy, is intrinsic to the material; all other anisotropies are induced. In crystal anisotropy, the ease of obtaining saturation magnetization is different for different crystallographic directions. An example is a single crystal of iron for which Ms is most easily obtained in the [100] direction, then less easy for the [110] direction, and most difficult for the [111] directions. These directions and magnetization curves for iron are given in Figure 6.15. The [100] direction is called the easy direction, or easy axis, and because the other two directions have an overall smaller susceptibility, the easy axis is the direction of spontaneous magnetization when below Tc. Both iron and nickel are cubic and have three different axes, whereas

FIGURE 6.15 Magnetization curves for single crystals of iron, cobalt, and nickel along different directions. Kittel, Introduction to Solid State Physics, 7E.

cobalt is hexagonal with a single easy axis perpendicular to the hexagonal symmetry (the c-axis). Figure 6.15 also gives magnetization curves for cobalt and nickel.

One may now imagine a situation in which the system has spontaneous magnetization along the easy axis but a field is applied in another direction. Redirection of the magnetization to be aligned with the applied field requires energy (through the change in M • H), hence the crystal anisotropy must imply a crystal anisotropy energy given by Equation (6.34) for a uniaxial material. This energy is an intrinsic property of the material and is parametrized, to lowest order, by the anisotropy constant K = K1 which has units of erg per cm3 or gram of material. Roughly speaking K1 is the energy necessary to redirect the magnetization. Table 6.7 gives values for a number of materials. For a uniaxial material with only K1, one can show (see below) that the field necessary to rotate the magnetization 90° away from the easy axis is

H = 2K1 /Ms

$$H = 2K_1/M_s \qquad\qquad (6.35)$$

Similar expressions with H ~ K1 /Ms apply to cubic systems. As an example, consider uniaxial cobalt with Ms from Table 6.3 and K1 from Table 6.7, one

TABLE 6.7 Anisotropy constants,

K1

Compiled from references 1 and 3.

calculates H = 6300 Oe to saturate 90° from the easy axis. In fact, the experimental value is — 12,000 Oe because in cobalt a higher order anisotropy constant, K2, makes a contribution to this recalcitrance.

The physical origin of the magnetocrystalline anisotropy is the coupling of the electron spins, which carry the magnetic moment, to the electronic orbit, which in turn is coupled to the lattice. Recall it was the strong coupling of the orbit to the lattice via the crystal field that quenched the orbital angular momentum.

6.4.1.2   Shape Anisotropy It is easier to induce a magnetization along a long direction of a nonspherical piece of material than along a short direction. This is so because the demagnetizing field is less in the long direction, because the induced poles at the surface are farther apart. Thus, a smaller applied field will negate the internal, demagnetizing field. For a prolate spheroid with major axis c greater than the other two and equal axes of length a, the shape anisotropy constant is

Ks = 2(Na - Nc)M2   (6.36)

where Na and Nc are demagnetization factors. For spheres, Na = Nc because a = c. It can be shown that Nc + 2Na = 4re; then in the limit c ^ a, that is, a long rod, Ks = 2tcM2 . Thus a long rod of iron with Ms = 1714

$$K_s = \frac{1}{2}(N_a - N_c)M^2 \qquad\qquad (6.36)$$

emu cm-3 would have a shape anisotropy constant of Ks = 1.85 x 107 erg cm-3. This is significantly greater than the crystal anisotropy, see Table 6.7, so we see that shape anisotropy can be very important for nonspherical materials.

6.4.2 Magnetic Domains

An ordinary piece of iron at room temperature is well below its Curie temperature, thus the exchange energy can align neighboring atomic moments so that they may act cooperatively to yield a macroscopic total moment. How is it then that this piece of iron in the absence of an applied field has no magnetic moment? The resolution to this paradox was given by Weiss in 1906, who proposed that a macroscopic magnetic material will break up into domains that align themselves in such a manner as to minimize the total effective moment of the material.

A magnetic field contains energy proportional to the field squared and its volume extent. Thus the magnetostatic energy of a single domain of parallel spins can be decreased by breaking it into smaller, oppositely aligned domains. This beneficial decrease in energy would continue with further breaking into more and yet smaller domains were it not for another energy that increases with declining size. This energy is the exchange energy at the boundary between oppositely aligned domains which, by the ferromagnetic nature of the

coupling, fights against the antialignment.

This competition between the magnetostatic energy and what we will call the domain wall limits the break-up of the material to domains of a finite size. This process is represented in Figure 6.16.

Hexagonal Cubic

FIGURE 6.16 Domain creation and the associated magnetostatic field for both hexagonal and cubic crystals. Note how the external field decreases, and hence the magnetostatic energy decreases, as the system breaks into domains.

The boundary between domains, the domain wall, is a result of another competition of energies. The exchange interaction between two antiparallel spins in a ferromagnet is so unfavorable that the material tends to develop a wall of finite thickness, so that the 180° difference in spin alignments between domains can be shared by many spins as depicted in Figure 6.17, and hence a thick wall is favored. However, only the two antiparallel spins are along the material's easy axis, so that those in the finite thickness wall are tipped away from the easy axis. This gives rise to the magnetocrystalline anisotropy energy, which is not favorable and hence tends to minimize the thickness of the wall. This competition leads to an optimal

$$l \simeq \sqrt{kT_c/Ka} \qquad (6.37)$$

$$\gamma \simeq \sqrt{kT_cK/a} \qquad (6.38)$$

wall thickness given approximately by

$$I \quad - \text{sj } kTc/Ka \qquad (6.37)$$

with a surface energy of

$$y - \text{sj } kTcK /a$$

FIGURE 6.17 Depiction of the spin orientation rotation through the domain (Bloch) wall. Kittel, Introduction to Solid State Physics 7E. Copyright© 1995 John Wiley & Sons, Inc. Reprinted by permission of John Wiley & Sons, Inc.

where a is the lattice spacing. Typical values are domain walls of a few hundred angstroms thick with energy on the order of 1 erg cm-2.

Domains can be observed via a number of techniques including the Bitter method, which involves treating the surface of the magnetic material with colloidal Fe304, Lorentz microscopy with a transmission electron microscope, and optical polarization methods using either the Kerr or Faraday effects.1

6.4.3 Hysteresis

When a ferromagnetic material is magnetized by an increasing applied field and then the field is decreased, the magnetization does not follow the initial magnetization curve obtained during the increase. This irreversibility is called hysteresis. An example of a full or major (i.e., M is taken to near Ms) hysteresis curve (or loop) is given in Figure 6.18. At extremely high applied fields, the magnetization
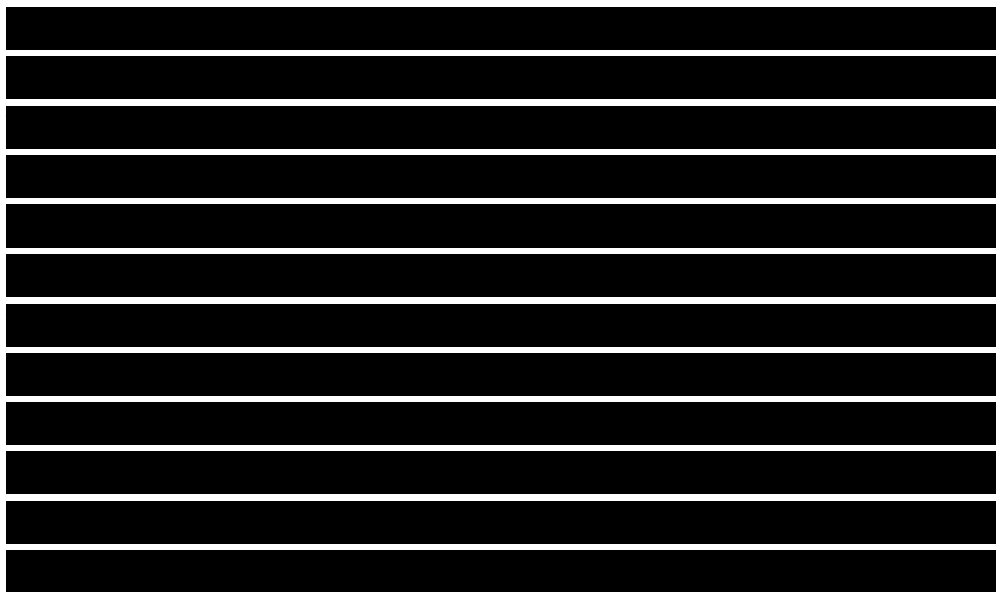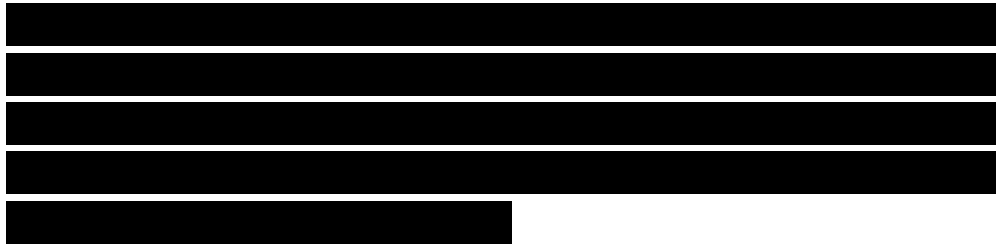
approaches the saturation magnetization, Ms. Then if the field is decreased to zero, the M versus H curve does not follow the initial curve but instead lags behind until, when $H = 0$ again, a remanant magnetization remains, the remanence Mr. If the field is now applied in the reverse direction (a negative field), M is forced to zero at a field magnitude called the coercivity, Hc. Increasing this negative field still further forces the magnetization to saturation in the negative direction. Symmetric behavior of this hysteresis curve is obtained as H is varied widely between large positive and negative values. 0ne could say that hysteresis is due to internal friction. Hence the area inside the loop is the magnetic energy that is dissipated while circling the loop. M

FIGURE 6.18 A full-loop hysteresis curve. Ms is the saturation magnetization, Mr is the magnetization remanence (at $H = 0$), and Hc is the coercivity.

Cardinal points along the hysteresis curve are Ms, Mr, and Hc. Permanent magnets used in motors, generators, loudspeakers, and "refrigerator magnets'' require large Ms and Mr. It is also desirable that permanent magnets not be easily demagnetized by unexpected fields, hence a large coercivity is good as well. Materials with $H_c > 100$ Oe are called hard magnets. The
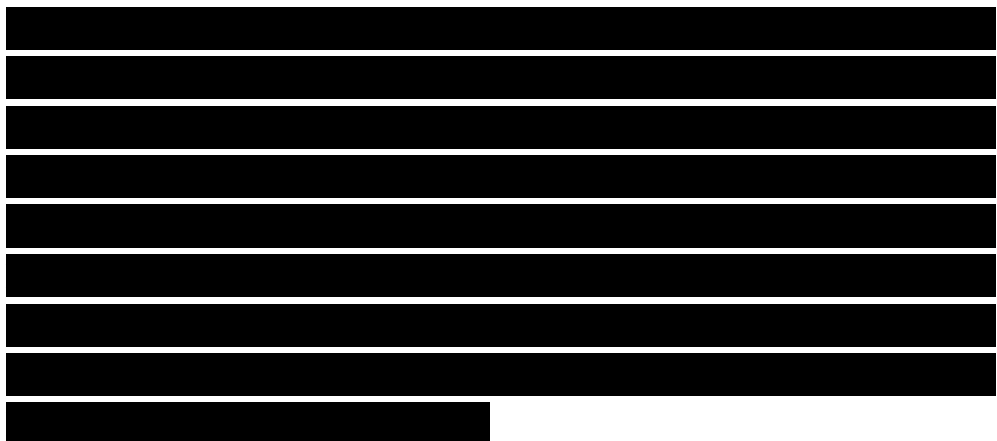
combination of large Mr and Hc can be parametrized by the energy product, which is the maximum value of M • H in the second (demagnetizing) quadrant of the hysteresis curve.

Soft magnetic materials are those with small Hc, typically Hc < 10 Oe. (The boundary between hard and soft is somewhat arbitrary and indefinite). Soft materials are needed for transformer cores because in AC applications the hysteresis loop is circled 60 times a second and, since the area of the loop represents dissipated energy, this energy is lost with every cycle. Other applications for soft materials are in electronic circuits.

The initial magnetization curve starting from the origin at (H, M) = (0, 0) has a number of interesting features shown in Figure 6.19. Overall, the curve may be divided into two regimes. A schematic representation of the magnetization process is shown in Figure 6.20. Initially, when H = 0, Figure 6.20 shows a ferromagnetic sample with two domains each with the saturation magnetization along the easy axes but in opposite direction so that in total M = 0. As a finite field is applied, at some small angle relative to the easy axis, the domain less aligned with the field dimin¬ishes in favor of the one more aligned via domain wall motion to the right. This process causes the magnetization to increase in a parabolic manner concave upward, as shown in
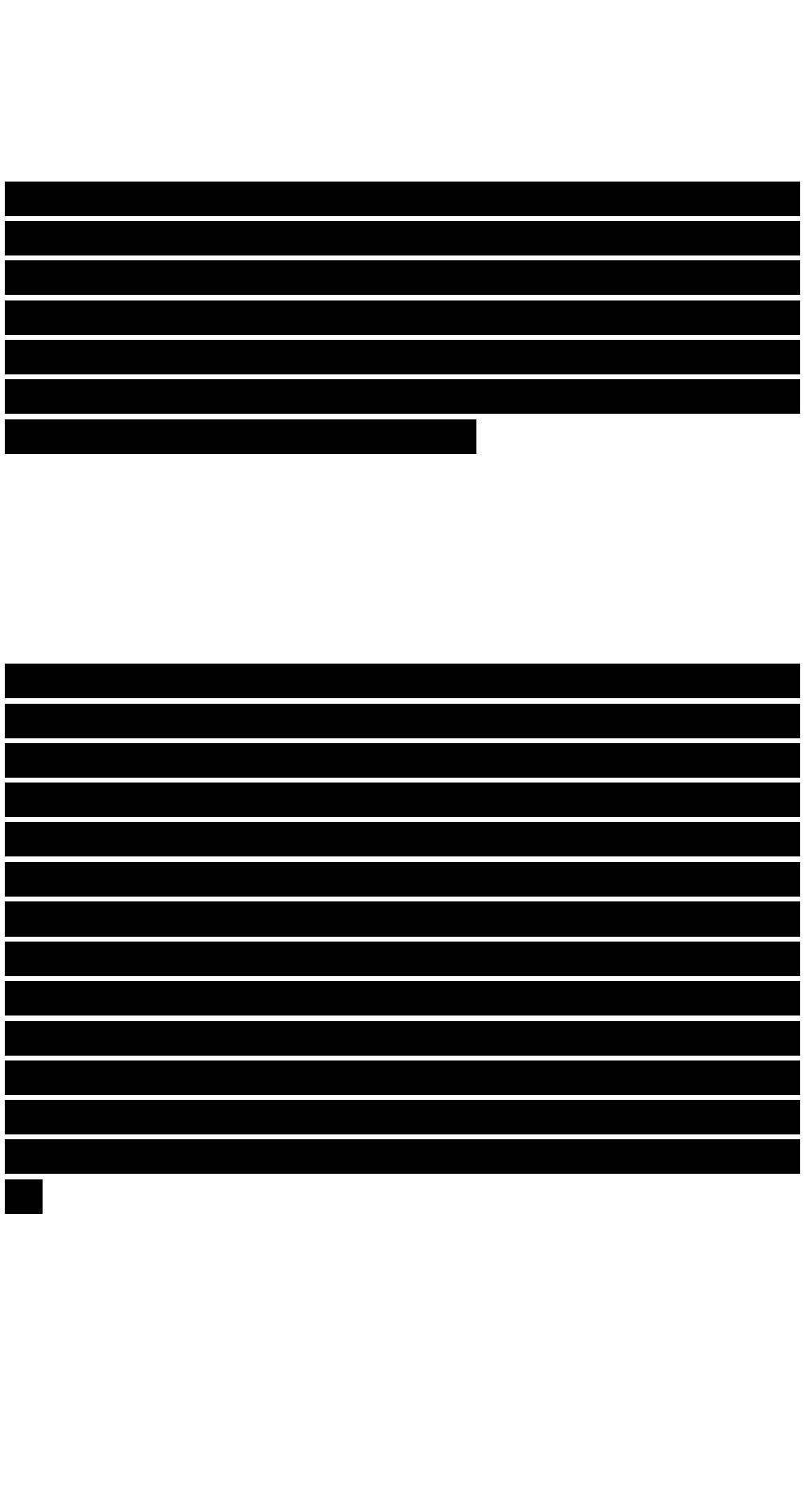
Figure 6.19. This continues until the sample is one domain. Further increase of the component of Ms along the direction of the applied field H requires

FIGURE 6.19 Initial magnetization curve showing regions of domain wall motion and the Barkhausen effect and magnetization rotation.

rotation of the Ms vector away from the easy axis. Thus at high fields, this curve bends over to yield a knee in the curve also shown in Figure 6.19.

Detailed description of the low-field behavior of the initial magnetization is given by the Rayleigh law, which describes the permeability p as

p = p0 + vH (6.39)

In Equation (6.39), p0 and v are the Rayleigh constants of the material. These constants range widely, from 30 to 105 for p0 and from 0.5 to 1.2 x 107 for v, and depend on the material, temperature, and degree of cold work. Since B = pH,

B = p0H + vH2   (6.40)

hence the parabolic nature of M versus H at low H.

In the regime of domain wall motion due to changing H, the magnetization is found to change not continuously but rather in a series of very small jumps. This is called the Barkhausen effect. A magnified view of the M versus H curve shows M varying like a random staircase (Figure 6.19). This Barkhausen effect is due to

$$\mu = \mu_0 + vH \qquad (6.39)$$

$$B = \mu_0 H + vH^2 \qquad (6.40)$$

the domain walls sticking at inclusions as they attempt to move with changing H.

At large fields, past the knee in the M versus H curve when M is rotating against the anisotropy, the behavior of M can be well described by the law of approach to saturation:

$$M(H) = M_s(1 - a/H) \qquad (6.41)$$

This can be useful for experimental determination of Ms in materials that are hard to saturate since extrapolation of M versus H-1 is linear and at H-1 ^ 0 the extra¬polation is Ms.

6.5 SMALL-PARTICLE MAGNETISM

The magnetism of small ferromagnetic particles (e.g., 1 or less) is dominated by two key features:

• There is a size limit below which the specimen can no longer gain a favorable energy configuration by breaking up into domains, hence it remains with one domain.

• The thermal energy can, with small enough size, decouple the magnetization from the particle itself to give rise to the phenomenon of superparamagnetism.

These two key features are represented by two key sizes (or length scales), the single domain size and the superparamagnetic size, each of which is described below.

6.5.1 Single-domain Particles

We saw above how the magnetostatic energy of a ferromagnet could be decreased

by restructuring the material into domains. There is a limit to this because formation of domains costs energy due to domain wall formation. Thus in a large body there could be a minimum domain size below which the energy cost of domain formation exceeds the benefits from decreasing the magnetostatic energy. This further implies that a single particle of size comparable to the minimum domain size would not break up into domains.

This scenario does indeed occur because of the different functionalities with size of the two competing energies. For a particle of size D (diameter) the magnetostatic energy is proportional to Ms2D3 because (1) the energy density in the field goes as B2 hence Ms2, and (2) the total energy is the energy density times a volume, hence the D3 proportionality. Domain formation requires creation of walls, which are an area. Hence if y is the domain wall energy per unit area, we expect a yD2 functionality for the total domain wall energy. Now consider large D, then the D3 term of the magnetostatic energy dominates, so to alleviate this the smaller D2 term of wall formation concedes and domains form. However, at small D, the D2 term will dominate and wall formation will be too costly and the particle will not break into domains. The critical size, or single domain size Ds, below which a particle will not form domains, is where these

$$D_s \sim \gamma/M_s^2 \qquad (6.42)$$

two energies are equal. If we ignore proportionality constants, this implies yD^ — Ms2D3 to yield

Ds - y/Ms2 (6.42)

This result (essentially a dimensional analysis) is surprisingly accurate (good to an order of magnitude). Typical values for Ds range from 10 to 100 nm, as shown in Table 6.8,6 with elongated particles tending to have large Ds.

6.5.2 Coercivity of Single-domain Particles

Magnetization reversal in single-domain particles must occur via spin rotation since there are no domain walls to move. Because of this, single-domain particles have a larger coercivity compared to multidomain systems because, generally speaking, it is harder to rotate the magnetization than to move a domain wall.

Most simply, magnetization can rotate by coherent motion of the atomic spins, but other motions—fanning and curling—can occur. We consider each below.

6.5.2.1 Coherent Rotation of the Magnetization

If the spins move coherently together, then they can be represented collectively by Ms. The response of Ms to an applied field is hindered by the anisotropy (crystalline, shape, stress, or whatever) and for coherent rotation was first considered by Stoner and Wolfarth. The lowest-order and simplest term in the anisotropy energy is given by Equation (6.34),
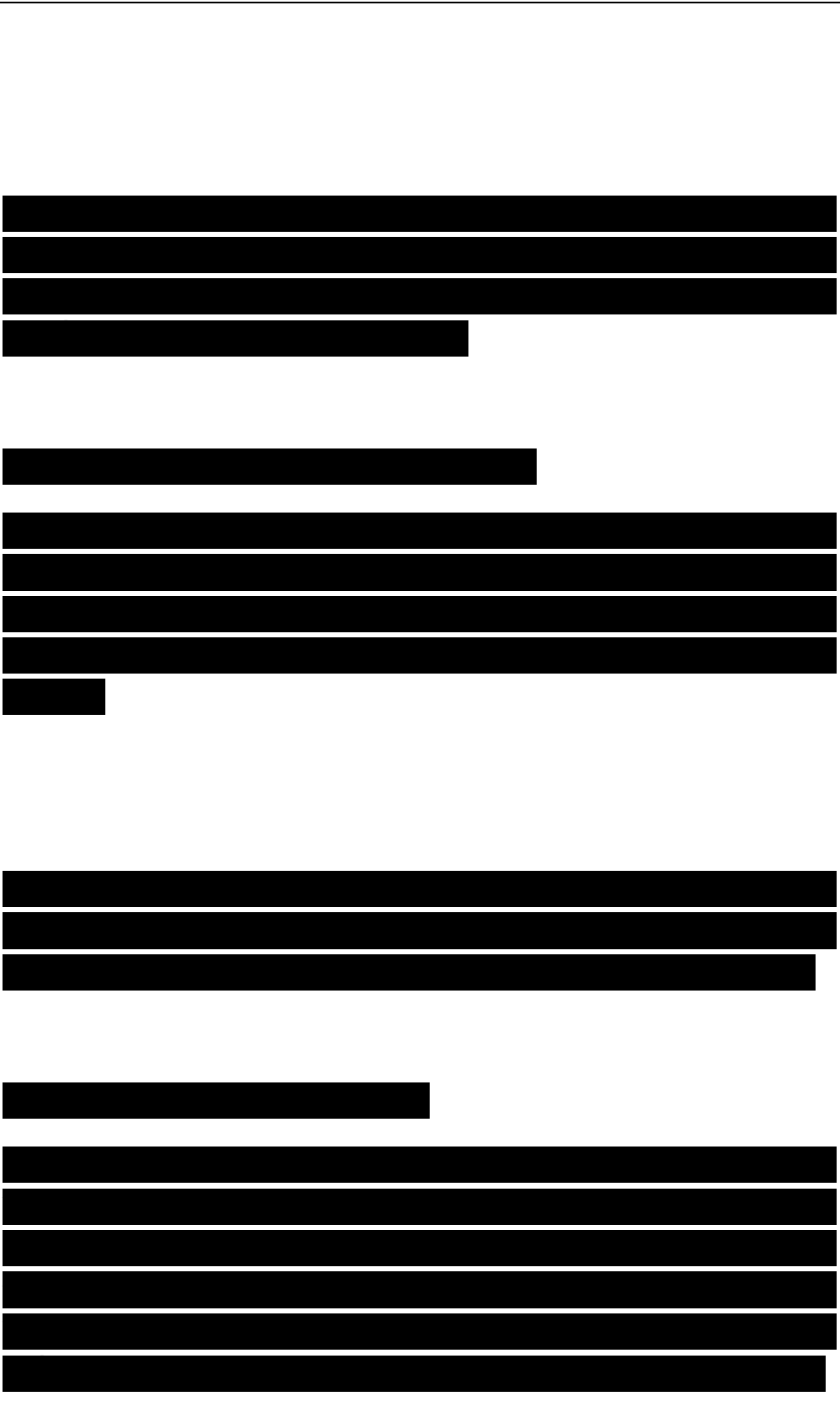
$$E_a = K \sin^2 \theta \qquad (6.34)$$

Ea = K sin2 d   (6.34)

TABLE 6.8 Estimated single-domain size for spherical particles

The applied field supplies a potential energy of

Ef = -Ms • H   (6.43)

$$E_\mathrm{f} = -\vec{M}_\mathrm{s} \cdot \vec{H} \qquad\qquad (6.43)$$

The equilibrium direction of Ms is where the total energy, Etot = Ea + Ef has a minimum. To find this, one differentiates and sets dEtot/d6 = 0.

Consider the situation in which the applied field is perpendicular to the easy axis. Then the field alignment energy is — MsH sin 6 and a minimum in Etot is found at sin 6 = MsH/2K. Thus the component of Ms parallel to the applied field, Ms sin 6, is proportional to H. Since sin 6 < 1, this component saturates to Ms when

H = 2K /Ms (6.44)

$$H = 2K/M_\mathrm{s} \qquad\qquad (6.44)$$

M versus H for this case is shown in Figure 6.21.

Now consider when H is applied antiparallel to Ms, which is along the easy axis, in an attempt to reverse the direction of Ms. In this case H applies no torque and so Ms is not even slightly rotated, so M = Ms remains. However, with increasing H, the magnetic energy for reversal, MsH, eventually becomes great enough that the minimum in the total energy shifts from the original Ms antiparallel to H to Ms parallel to H at H = 2K/Ms. The system makes this jump and this leads to

a square hysteresis curve, also shown in Figure 6.21, with coercivity given by Equation (6.44).

So far we have only considered the situations where the applied field is perpendicular or antiparallel to Ms along the easy axis. Other initial orientations can be attacked in the same manner, viz., minimization of the total energy. One finds that the two cases we have considered represent extremes of the possible hysteresis curves, totally closed (no hysteresis) and totally open (square). Other orientations

FIGURE 6.21 Hysteresis loops for applied fields perpendicular ± and parallel || to the easy axis.

FIGURE 6.22 Hysteresis loops for field applied to an ensemble of uniaxial, single-domain particles with random easy axes.

yield hysteresis curves between these limits. Very often when dealing with particles, the easy axes are randomly oriented. Then a hysteresis curve results that is an average over all orientation. This average is shown in Figure 6.22.

We have not yet considered the source of the anisotropy K. It could occur due to crystalline anisotropy, shape, stress, or, in small particles, to surface anisotropy. Table 6.9 contains calculated coercivities Hc = 2K/Ms for iron due to the shape anisotropy. There we see a typical result that for even modest shape
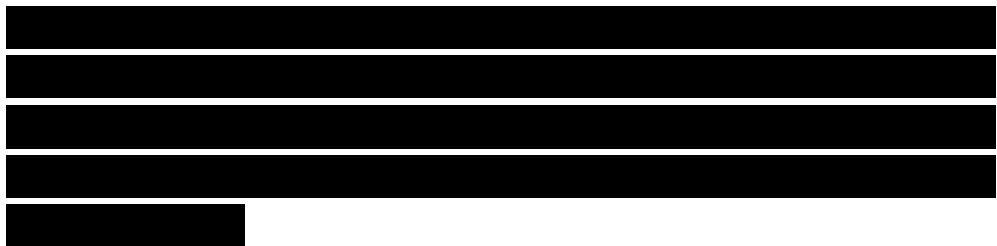
ratios, c/a, the shape anisotropy can be very large. This can be shown to be true for stress aniso¬tropy as well. Thus for particles, shape can dominate the coercivity.

TABLE 6.9 Calculated shape anisotropies (Equation 6.36) and coercivities (Equation 6.44) (easy axis aligned with field) for single-domain iron particles (Ms = 1714 emu cm-3)

6.S.2.2 Fanning

Magnetization reversal by the fanning mechanism is relevant in chains of particles or highly elongated particles. In a chain the Ms vector of each particle interacts with its neighbors via the magnetic dipolar interaction. Thus the dipoles line up, north to south, and like to remain in alignment, hence causing an anisotropy even if no others exist. This has been called an interaction anisotropy. An applied field in the opposite direction tends to reorient these dipoles, but the re¬orientation may occur either coherently as depicted in Figure 6.23 or incoherently also depicted in Figure 6.23. The incoherent realignment is called fanning.

Fanning reversal leads to a square hysteresis loop. The Hc is one-third as large as for a coherent reversal and can be calculated to be

Hc (fanning) = n'Ms/6

Equation (6.45) works fairly well for some real systems, even in situations where the approximation of a chain of

$$H_c(\text{fanning}) = \pi M_s/6 \qquad (6.45)$$

pointlike particles used to derive (6.45) is poor, for example, in highly elongated particles.

6.5.2.S   Curling To visualize magnetization reversal by curling, place the initial magnetization along positive z-axis and imagine each atomic spin rather than the total Ms. Next apply a field H along the negative z-axis in an attempt to reverse the total Ms. Now consider an xj plane slice of this, depicted in Figure 6.24. As the total Ms turns to reverse, the atomic spins could either stay parallel so that their xj components are equal—this would be coherent rotation as in Figure 6.24a—or they could rotate away from the z-axis with different xj components. If these xj components are always perpendicular to a radius vector in the xj plane as in Figure 6.23b, this is called curling.

For an infinitely long particle, the energy barrier to reversal via curling is entirely exchange. The logic to this can be seen in Figure 6.24b, which shows how the atomic spins are not parallel, so that exchange energy is involved, and are parallel to the surface, so that there are no poles on the surface, hence there is no magnetostatic

FIGURE 6.23 Schematics of coherent and fanning rotation of magnetization in particles, initially upward, with an applied field downward.

energy. For finite lengths, the magnetostatic energy becomes important as well. Curling has a
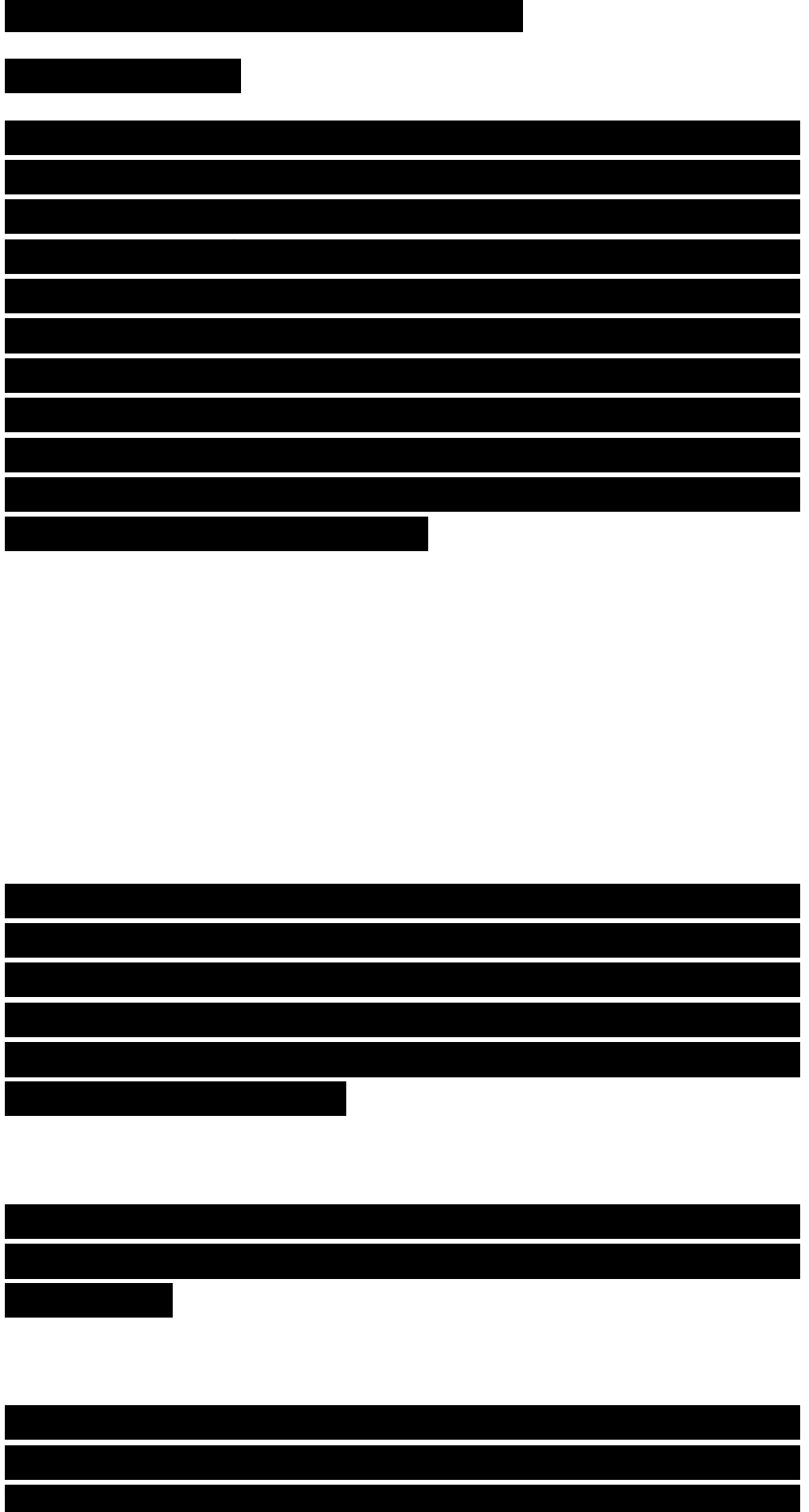
size dependency because smaller particles force the average angle between adjacent atomic spins to be greater, hence the exchange is more effective in resisting the reversal. It is for this reason that small particles reverse coherently, whereas large particles use curling. For iron this crossover occurs at roughly 15 nm.

6.5.3 Superparamagnetism

Below the Curie temperature of a ferromagnet or ferrimagnet, all the spins are coupled together and so cooperate to yield a large total moment. This moment is bound rigidly to the particle by one or more of the variety of anisotropies that we have discussed, and the energy of this bond is KV, where V is the volume of the particle. With decreasing particle size, KV decreases until the thermal energy kT can disrupt the bonding of the total moment to the particle. Then this moment is free to move and respond to an applied field independent of the particle. This moment is the moment of the particle and is equal to pp = Ms V. It can be quite large, thousands of Bohr magnetons. An applied field would tend to align this giant (or super) moment, but kT would fight the alignment just as it does in a paramagnet. Thus, this phenomenon is called superparamagnetism.

If the anisotropy is zero or very weak, one would expect that the total moment pp = Ms V could point in any direction, hence the Langevin function of Equation

(6.16) would apply. If K is significantly greater than zero, p could appoint in either of the two directions along the easy axis and then the two-state Brillouin function would apply (Equation 6.23). Both of these, however, are an approximation to M

versus H for a real superparamagnet because the system of particles is no doubt polydisperse, so that there is a distribution of ^p values, and the particles would most likely have random orientation, hence random easy axes. Despite this lack of a precise qualitative description of M versus H, two key qualities remain for a superparamagnetic system: (1) lack of hysteresis, and (2) data of different temperatures superimpose onto a universal curve of M versus H/T. Both these features are illustrated in Figure 6.25.

The phenomenon of superparamagnetism is, in fact, timescale-dependent due to the stochastic nature of the thermal energy. The anisotropy energy KF represents an energy barrier to the total spin reorientation; hence the probability for jumping this barrier is proportional to the Boltzmann factor exp(-KF/AT). This can be made quantitative by introducing an attempt timescale T0, which describes the timescale over which ^p attempts to jump the KF barrier. Then the timescale for a successful jump is

t = t0 e-KF/AT   (6.46)

The attempt timescale is about

$$\tau = \tau_0 \, e^{-KV/kT} \qquad (6.46)$$

10-9 s. The typical experiment with a magnetometer takes 10 to 100 s; and if Ms reverses at times shorter than the experimental time- scales, the system appears superparamagnetic. Using t ~ 100 s and t0 = 10-9 s, one obtains from (6.46), for the critical volume,

$$V_{sp} = 25kT/K \tag{6.47}$$

Fsp = 25 AT/K   (6.47)

A particle with volume smaller than this acts superparamagnetically on the 100 s experimental timescale. Typical superparamagnetic sizes for spherical (magneto¬crystalline anisotropy only) iron and cobalt particles are 16 and 7.6 nm, respectively, for T = 300 K.

FIGURE 6.25 Magnetization for very small, ~ 0.6 nm, cobalt particles. (a) Data are plotted versus applied field H; (b) the same data plotted versus H/T. The collapse of the data to a single curve in (b) indicates superparamagnetism. J P Chen, C M Sorenson, K J Klabunde and G C Hadjipanayis. In: Mafen'a/s, edited by G C Hadjipanayis and R W Siegel, Kluwer Dordrecht, 1994, with kind permission from Kluwer Academic Publishers.

Equation (6.47) can be rearranged to yield

$$T_B = KV/25k \tag{6.48}$$

Tb = KV/25k

Tb is called the blocking temperature; below TB the free movement of pp = Ms V is blocked by the anisotropy; above TB, kT kicks the moment loose so

that the system appears superparamagnetic.

We have seen above, when discussing single-domain particle hysteresis, that an applied field can modify the anisotropy energy barrier. One then finds that for the experimental timescale of 100 s superparamagnetism begins when HMs\

25kT = KV| 1 - j

$$25kT = KV\left(1 - \frac{HM_s}{2K}\right)^2 \qquad (6.49)$$

Solving this for T, a new, and lower at finite H, blocking temperature TB can be calculated. Essentially the applied field is lowering the KV barrier so that super¬paramagnetism begins at a lower T. If one solves for H, one obtains the coercivity for small single-domain particles in the size regime immediately above the super- paramagnetic size:

Recall that 2K/Ms is the coercivity without the help of thermal activation. Since Vp = 25kT/K, and V ~ D3, one finds

On the other hand, if Equation (6.48) is used with (6.50), one finds

This temperature functionality is illustrated in Figure 6.26.

The importance of the timescale dependency of superparamagnetism is well illustrated by Mossbauer experiments on magnetic particles. If the system of parti¬cles is ferromagnetic, a sextet of Mossbauer lines is observed, whereas if the system is superparamagnetic, a doublet is observed. The gamma-ray interaction of the

Diameter: ■, 44A; •, 56A; A,
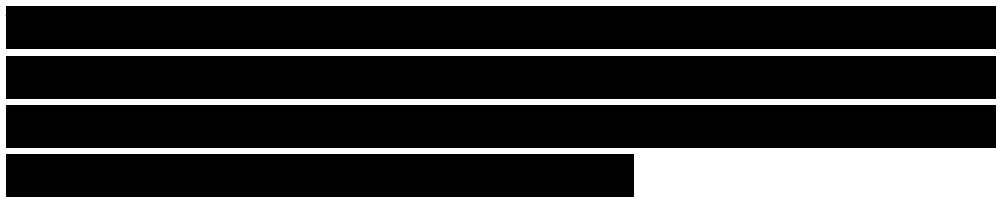
64A;T, 88A

Mossbauer experiment works on a very quick timescale, on the order of 10-7 s. Thus by Equation (6.46) one expects

Tb (Mossbauer) ^55
TB (Magnetometer)

$$\frac{T_{\mathrm{B}}(\text{Mössbauer})}{T_{\mathrm{B}}(\text{Magnetometer})} \simeq 5.5 \tag{6.53}$$

Dp (Magnetometer)
(6.54)

$$\frac{D_{\mathrm{P}}(\text{Mössbauer})}{D_{\mathrm{P}}(\text{Magnetometer})} \simeq 0.6 \tag{6.54}$$

The blocking temperature can be easily measured in the laboratory with a magnetometer. With TB, one can then infer values for the particle size, anisotropy, or saturation magnetization through Equation (6.48). The procedure is to cool the sample under zero applied field, so-called zero-field cooling (ZFC), to a temperature well below the suspected TB. Then apply a small field of ~ 100 Oe. If T < TB, the individual particle's moments are bound to the particles, point in random directions, and will not be very susceptible, so the induced magnetization will be small. The system is then warmed at a uniform dT/dt. As T approaches TB from below, kT will begin to loosen up the moments from the particles and the induced M will rise. At Tb, the moments are unblocked and hence are free to align with the applied field to yield a large total M. As T increases above TB, M falls via the Curie law, M ~ T-1 because the system is a

(super)paramagnet. Thus a peak occurs at TB. An example of this is given in Figure 6.27. Another example is given in Figure 6.28, which shows that TB is modified when the particles interact via the magnetic dipole interaction.

The data in Figure 6.27 are for cobalt particles synthesized in our laboratory. Their diameters were measured with a transmission electron microscope. The total moment ^{p} was determined by fits to the Langevin function for T > TB, and the effective anisotropy and saturation magnetization were determined from all these with Equation (6.48). The results are shown in Table 6.10.

6.5.4 The Coercivity of Small Particles

We can pull together much of the discussion above into Figure 6.29 which gives a schematic of the coercivity as a function of particle size. At large size the particles have many domains; thus, magnetization reversal is dominated by domain wall motion, which is relatively easy, hence the coercivity is low. However, as particle size decreases, the coercivity is found empirically to follow

FIGURE 6.27 Magnetization versus temperature for small cobalt particles. The particles were zero-field cooled and then warmed under an applied field of 100 Oe. Peaks in the data curves indicate the blocking temperatures. Lines are high-T fits to the Langevin function. Used with permission from J.
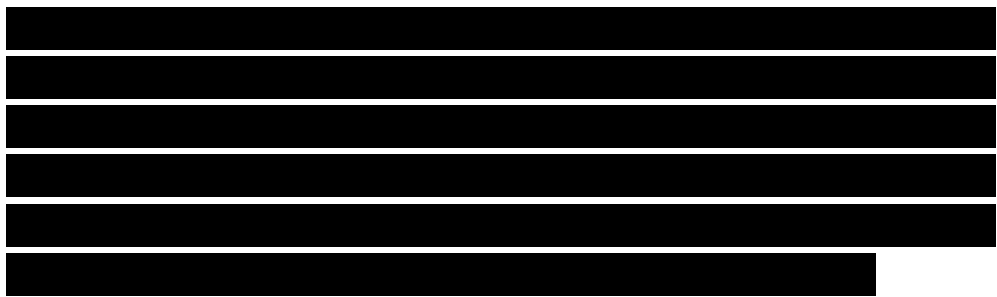
FIGURE 6.28 As in Figure 6.26, but when the particles are not diluted, the blocking temperature appears higher due to interparticle magnetic dipole interaction. Used with permission from J. Mater. Res., 14, 1542, 1999, Materials Research Society.

until the single-domain size is reached. Equation (6.55) is not well understood theoretically. The largest coercivities occur at the single-domain size. Below this, Hc falls off due to thermal activation over the anisotropy barriers, leading to Equation (6.52) and superparamagnetism at the superparamagnetic size for which Hc = 0.

The behavior represented in Figure 6.29 is shown for a real system in Figure 6.30. The system is iron encapsulated in magnesium prepared in our laboratory.5 For T > 77 K the coercivity rises from zero at D < 4nm, the superparamagnetic regime, and peaks near D = 20 nm. This peak size is in reasonable accord with the theo-

TABLE 6.10 Size-dependent magnetic properties of cobalt nanoparticles

FIGURE 6.29 Particle coercivity versus size (~ diameter). Dsp is the superparamagnetic size; Ds is the single-domain size.

retical prediction for the single domain size, Ds ~ 14 nm, given in Table 6.8. For yet larger sizes, Hc falls and the overall shape of Hc versus D is the same as expected

from Figure 6.29. Note that for T = 10 K the particles with D ~ 3 to 5 nm that were superparamagnetic at 77 K no longer are, indicating a blocking temperature for these sizes between 10 and 77 K.

The properties of ultrafine or nanoscale particles has stimulated considerable interest in the recent past due to inherent scientific interest as well as great potential for development of novel and useful materials. Nanoscale particles display a wide variety of unusual behavior when compared to the bulk for two major reasons: finite size effects in which electronic bands give way to molecular orbitals as the size decreases; and surface/interface effects.

For magnetic properties it is largely the latter, surface/interface effects, which cause significant differences compared to the bulk. In a nanoscale particle the surface atoms/bulk atoms ratio is sufficiently large (~ 50% for diameter ~ 3nm) that surface/interface effects can dominate the magnetic properties. One useful point of view is that small particles represent surface matter in macroscopic quantities. For instance, 10 mg of 3 nm cobalt particles would contain 5 mg of surface cobalt.

Surface/interfacial effects may be classified along the following lines:

(1) Symmetry breaking at surface or interface causing changes of (a) band structure, (b)

atom coordination, and (c) lattice constant.

(2) Electronic environment/charge transfer at the interface with, for example, (a) ligands, (b) other metals, (c) insulators, and (d) semiconductors.

A considerable amount of new knowledge of size effects on intrinsic magnetic properties has come from work on gas phase clusters of atoms whose magnetic moments have been measured with Stern-Gerlach apparatus.7,8 Systems studied have included 3d transition metals iron, cobalt, and nickel; a 4d transition metal, rhodium; and rare earths gadolinium and terbium. Sizes ranged from several atoms per cluster up to a few hundred, the latter corresponding to particle diameters of

2 nm. The 3d transition metals showed superparamagnetic behavior (as expected) with enhanced (~30-40%) magnetic moments per atom as shown in Figure 6.31. Theory ascribes enhancement to changes in atomic coordination, symmetries, and/or lattice constants.9 Reduction may be a surface effect resulting in weaker exchange. An exciting discovery, stimulated by theory,10 is that rhodium (a 4d transition metal) clusters, Rhn, n = 9-31, are ferromagnetic.11 This is thought to arise because of reduced coordination and icosohedral symmetry. Of course, all these changes are ultimately due to the very small size of the
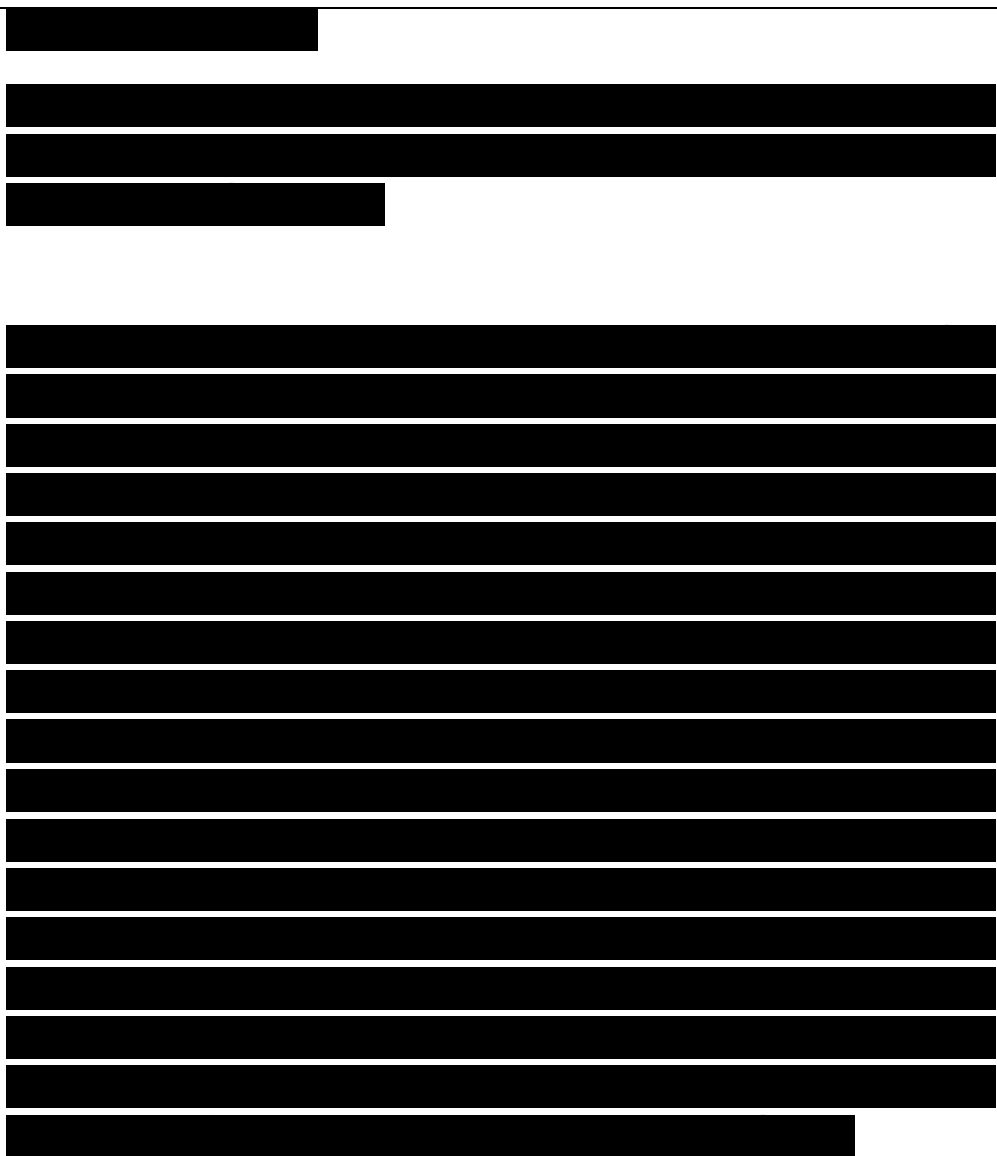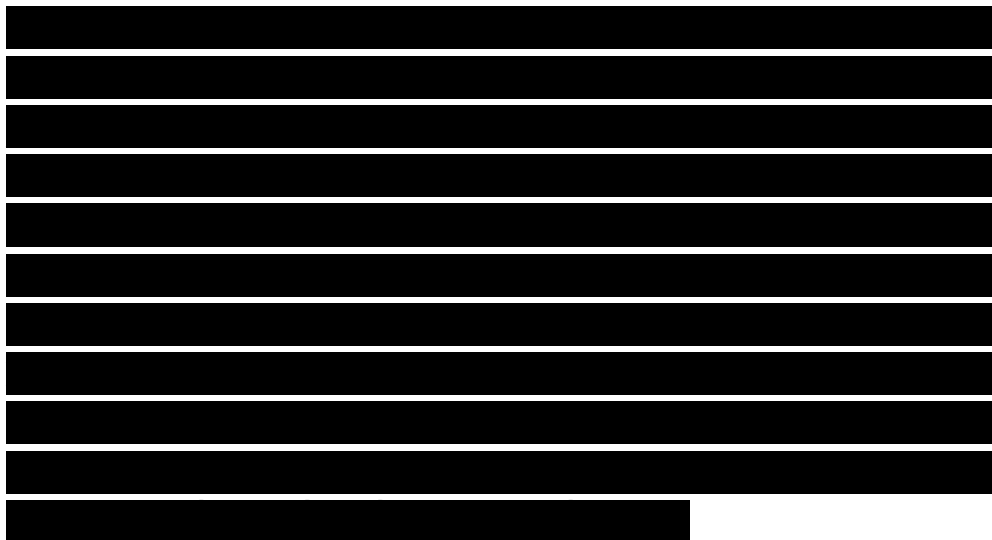
particle.

Small metallic clusters have also been incorporated into cluster compounds. For example, palladium clusters up to Pd561 with ligated phenyl and oxygen, Pd561Phen36O200, have been made.12 These compounds have never shown ferro¬magnetism but have shown interesting quantum size effects in their paramagnetic properties. Calculations indicate for palladium that a 5.5% lattice expansion would make it ferromagnetic.13 Why are rhodium gas phase clusters ferromagnetic yet palladium cluster compounds are not? The answer could have a lot to do with electron-donating ligands on the palladium cluster compound. For instance, Rosch et a/.14 studied nickel clusters and saw the ferromagnetism quenched as CO ligands

100 200 300 400 500 600 700 Cluster size OV)

FIGURE 6.31 Low-temperature average magnetic moment per atom for nickel clusters at 78 K, cobalt clusters at 78 K, and iron clusters at 120 K as a function of the number N of atoms in the cluster. The right-hand scale gives the spin imbalance per atom. Reprinted with permission from "Magnetic and Thermal Properties", In Proceedings of the Scientific and Technology of Atomically Engineered Materials, 1996, World Scientific Publishing Co Pte Ltd.

were attached. An example from our work is given in Figure 6.32

where it is shown that 4.4 nm cobalt particles ligated with dioctyl sulfide show a large reduction in the saturation magnetization. Thus, surface interactions are very important, and the Stern-Gerlach clusters are unique because they are not interacting with other substances. At the surface, the coordination number of each surface atom is smaller than within the bulk, hence the d-band of a collection of transition metal atoms at the surface is narrower than in the bulk, leading to a high density of states and hence enhanced magnetism.15-17 The surface magnetic moments are enhanced by 10-30% over their bulk values in ferromagnetic iron, nickel, and body-centered cubic cobalt (100) and (110) surfaces.16 A dramatic case is the chromium (001) surface, which undergoes a ferromagnetic phase transition, with an enhancement of about 3^B in its magnetic moment as compared to its bulk value (which is antiferromagnetic in nature).17,18 By contrast, the

FIGURE 6.32 Saturation magnetization of 4.4 nm cobalt particles with (A) and without (•) dioctyl sulfide ligation.

nature).17,18 By contrast, the results of experiments with vanadium (100) surfaces show a stable paramagnetic state for the surface and yield a 9% contraction of the topmost interlayer spacing.17 Experimental findings19 on thin
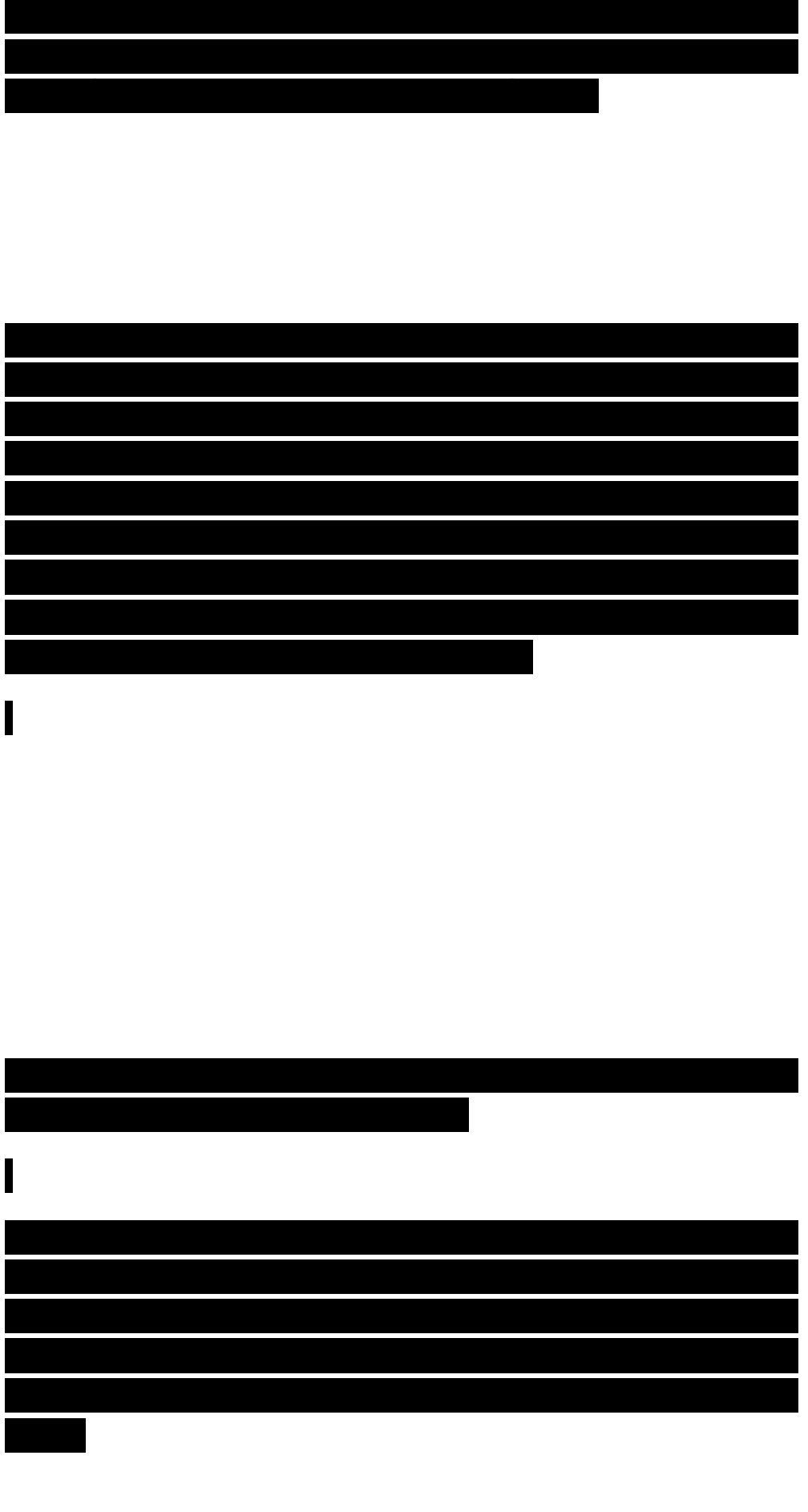
films of iron, nickel and cobalt show enhancements of surface moment by 30%, 20%, and 150%, respectively, as compared to their bulk.

Interfaces or small particles may have significant changes in the lattice constant relative to bulk. For example, a study of nanophase (d ~ 6nm) compressed iron showed two Mossbauer sextets that indicated the presence of both a bulk and an interfacial iron phase.[20] The overall density of the composite was ~ 75% of the bulk, indicating that the interfacial phase was less dense than the bulk. The interfacial iron had larger hyperfine fields and isomer shifts than bulk iron. The greater isomer shift was due to a smaller electron density. The enhanced hyperfine field was due to greater exchange, a result of moving to the right on the Bethe-Slater curve due to the greater lattice spacing in the expanded interfacial phase. Rayl et al.[21] cosputtered nickel and Si02 to create small nickel particles with a lattice constant increased by 9%. This caused a lowering of Tc, which correlated well with changes caused by high-pressure studies, which decrease the lattice spacing. Again this decrease in Tc, and hence exchange constant J_{ex}, correlates with the inference from the Bethe-Slater curve. Would an expanded interfacial phase of palladium show ferromagnetism? Analogously, an expanded lattice for chromium could yield ferromagnetism.
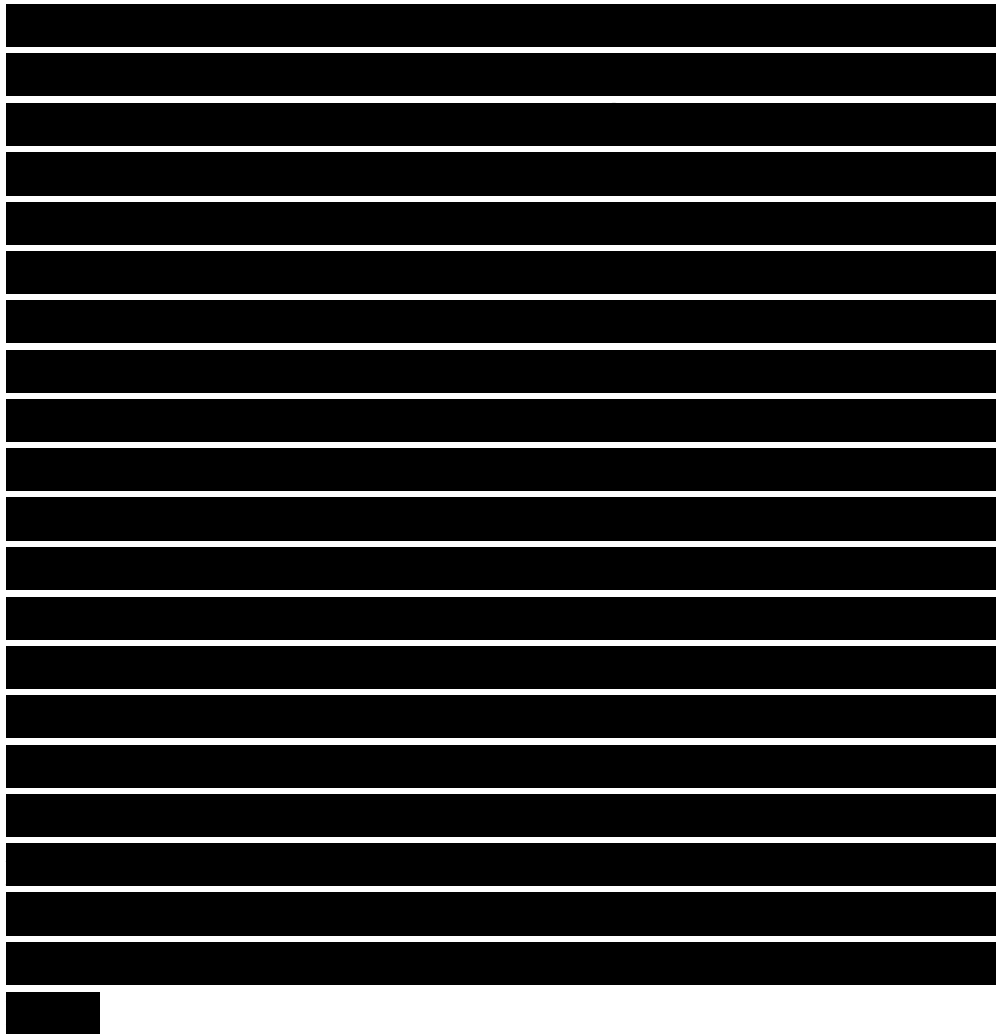
Could manganese be altered from antiferromagnetic to ferromagnetic in such an interfacial phase?

At an interface an adjacent metal may perturb the d-band. For example, copper on nickel decreases the moment per atom of nickel22 because copper donates electrons to the nickel d-band, thus partially filling the unpaired hole. On the other hand, iron next to silver sees an enhancement in ^ per atom.23 Similar opposing examples exist so the situation, while robust with phenomena, is very complex.24,25 One can glean from the literature that an important interfacial effect is the electronic interaction between adjacent materials. As discussed above, electron donation by ligands to palladium and cobalt and by both copper and nickel suppressed the magnetic moment in a straightforward manner. Other examples include cobalt particles precipitated in copper;26,27 iron particles in mercury;28 and our own work involving iron in MgF25 shown in Figure 6.33. This is very similar to the dioctyl sulfide ligand quenching for cobalt particles described above with, most likely, the same physics. Here we see that the smaller iron particles have smaller Ms. The quenching of Ms occurs due to donation of electrons from the MgF2, which surrounds the iron particle. The donated electrons partially fill the spin-unbalanced d-band of the iron, decreasing the
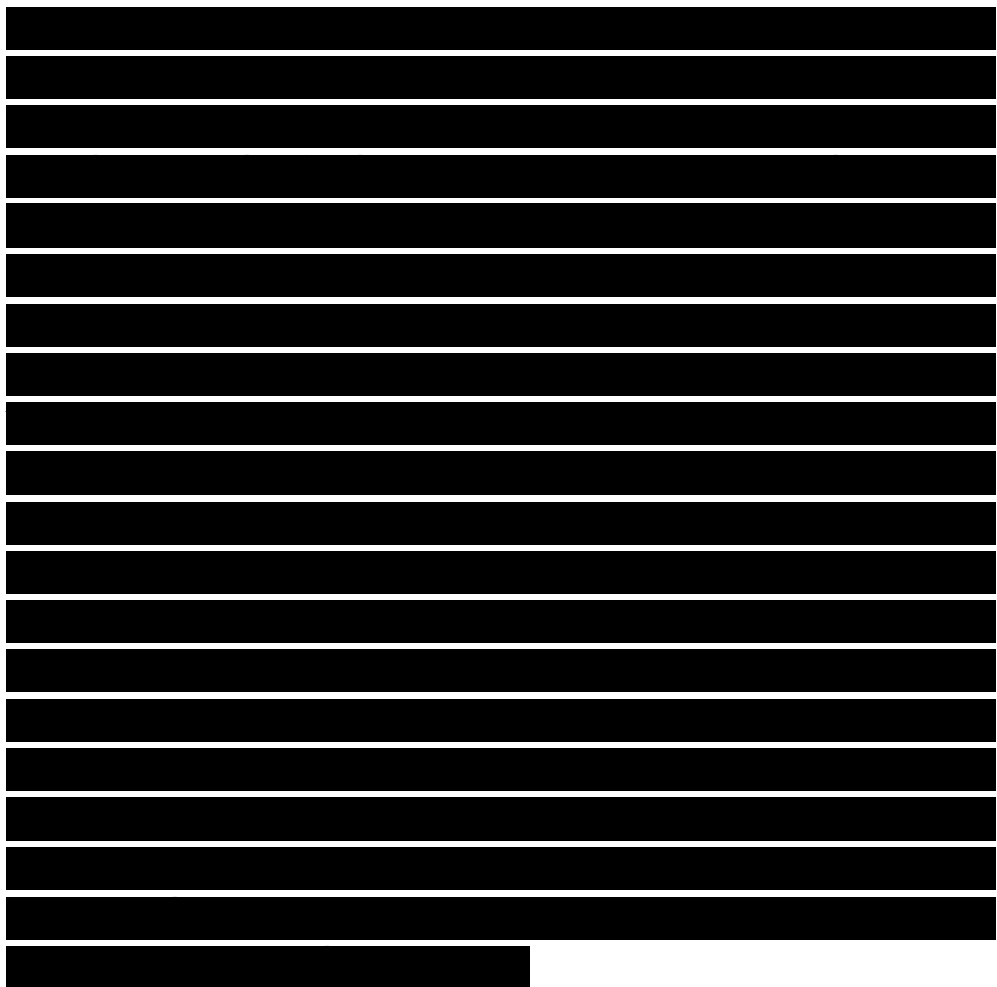
magnetic moment per atom. The larger quench for smaller particles is

due to the greater fraction of surface/interfacial iron. The relevant parameter is the electronegativity of the two substances. If the transition metal is more electro¬negative, it takes electrons and partially fills its d-band holes to become less magnetic, whereas if it is less electronegative, the reverse occurs. Such a proximity correlation does not appear to be discussed in the literature, but it is consistent with available data and the Slater picture of transition metal alloys29 discussed briefly above. Electronegativity is not important in Slater's picture because the metals are atomically mixed, but the simple concept of d-band hole filling with concomitant change in ^ per atom is the same as that used above.

In many situations particles display a dead layer on their surface in which the magnetization is either reduced or zero. This causes the total saturation magetization of the sample to be less than in the bulk, more so for smaller particles. If the layer is of constant thickness,

independent of the diameter of the particle, it is easy to show that then the magnetization is inversely proportional to the diameter. An example30 of this behavior is shown in Figure 6.34. The thermal behavior of the magnetization is also affected by the large fraction of surface material in nanoparticle systems. The data in Figure 6.8 for iron particles encapsulated in MgF2 show that the magnetization is decreased more by temperature for smaller particles. Analysis of these data, as well as data for iron encapsulated in magnesium, with Bloch's law showed that Bloch's law was still valid, but both the Bloch constant Bloch exponent were size-dependent, as shown in Figures 6.35 and 6.36. The large increase in B indicates that small-particle magnetization is very susceptible to temperature, most likely due to the reduced coordination of the iron atoms at the surface.5

Another common effect seen for nanoscale particles is surface anisotropy, that is, an (additional) energy binding the magnetization to the particle analogous to the crystal anisotropy. This occurs because the spins at the surface see the broken symmetry at the surface and this affects the spin alignment relative to the surface.

The hard magnetic properties of particles are also very important because of their potential applications in magnetic recording media. Coercivities in the range of a few

FIGURE 6.34 Saturation magnetization versus inverse mean particle diameter for MnOFe2O3 particles prepared by aerosol spray pyrolysis (solid symbols) and aqueous phase precipitation (open symbols). The lines are guides for the eye. From Aerosol Science & Technology: "Aerosol Spray Pyrolysis Synthesis of Magnetic Manganese Ferrite Particles". 19, 453-467. Copyright 1993. Cincinnati, OH. Reprinted with permission.

FIGURE 6.35 Bloch constant as a function of iron particle size. Iron particles are encap¬sulated in either magnesium or MgF2. Dashed line is bulk value. Reprinted with permission from D. Zhang et al, Phys. Rev. B, 1998, 58, 14167, American Physical Society.

Fe core diameter (nm)

FIGURE 6.36 Bloch exponent as a function of iron particle size. Iron particles are encapsulated in either magnesium or MgF2. Dashed line is bulk value. Reprinted with permission from D. Zhang et al, Phys. Rev. B, 1998, 58, 14167, American Physical Society.

kOe, which are much higher than the values of their bulk counterpart, have repeatedly been reported for the last 3-4 decades.

A magnetic coating material on a nanoparticle can have a dramatic effect on coercivity (often discussed in terms of exchange anisotropy1). Meikeljohn and Bean31 studied fine particles of cobalt metal with an outer layer

of CoO. An usually large Hc was explained in terms of exchange coupling between the spins of the ferromagnetic cobalt and antiferromagnetic CoO; thus the reversal of the spins of cobalt atoms in the cobalt core material was resisted by the strong crystal anisotropy of the CoO.

Analogous results were obtained in our laboratory32 for iron particles. Hc was found to increase with a decrease in particle size from 12 nm to 3nm, while <JS increased with increasing size. These results were explained by proposing that Hc is strongly affected by the interaction between the iron oxide shell and the iron core. The highest Hc obtained at room temperature was 1050 Oe for a particle with a 14.0 nm core, and its value at 10 K was 1425 Oe. However, smaller particles with 2.5 nm core size went from a negligible Hc at 150 K to 3400 Oe at 10 K, showing the much stronger influence of temperature on the smaller nanoparticles. It was proposed that the smaller iron core "feels" much more the effect of the iron oxide shell, due to the higher iron oxide/iron ratio. The strong decrease in Hc with temperature increase was explained as due to the onset of superparamagnetic behavior of the iron oxide shell.

An important conclusion is that surface coatings in such small particles can dominate Hc and can also control the temperature dependence. The coating spins
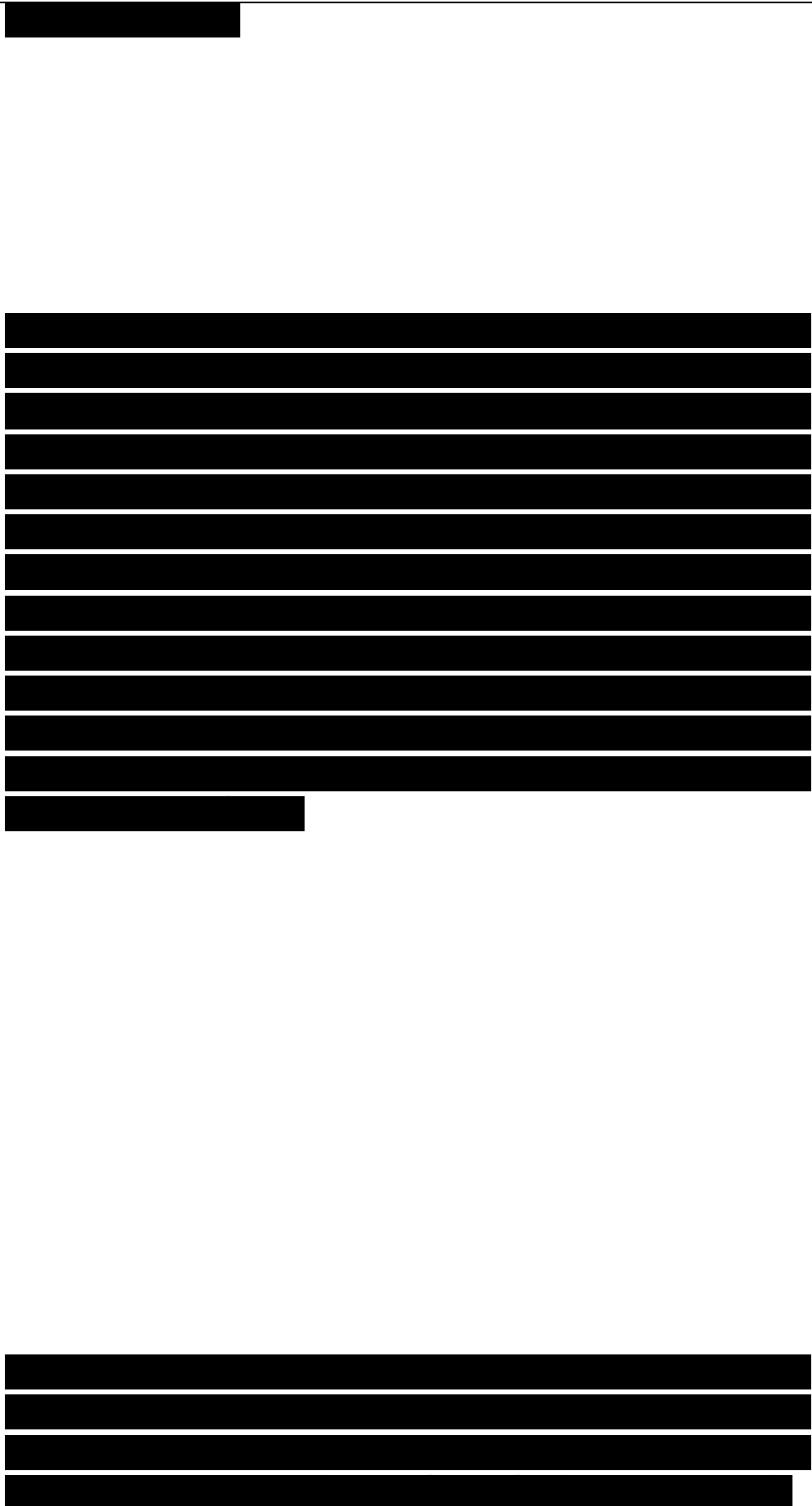
couple to the core via exchange, resulting in an exchange anisotropy.

GLOSSARY OF SYMBOLS

a   Lattice spacing
a   Minor axis of spheroid
b   Bloch exponent
B   Bloch constant
B   Magnetic induction (gauss)
Bj   Brillouin function
c   Major axis of spheroid
c   Speed of light
C   Curie constant
D   Diameter
e   Electron charge
Ea   Anisotropy energy
g   Lande g-factor
H   Magnetic field strength (Oe)